energies

MDPI

Article

Method for spatiotemporal solar power profile estimation for a proposed U.S.-Caribbean-South America super grid under hurricanes †

Rodney Itiki [1,*], Nils Stenvig [1], Teja Kuruganti [1] and Silvio Giuseppe Di Santo [2]

[1] Electrification and Energy Infrastructures Division, Oak Ridge National Laboratory, 1 Bethel Valley Rd, Oak Ridge, TN, 37830, USA; stenvignm@ornl.gov; kurugantipv@ornl.gov
[2] Dept. Energy and Automation, University of São Paulo, Av. Prof. Luciano Gualberto, travessa 3 nº 380 - São Paulo – SP, CEP, 05508-010, Brazil; silviogiuseppe@usp.br
* Correspondence: itikir@ornl.gov

† Acknowledgement: This manuscript has been authored by UT-Battelle, LLC, under contract DE-AC05-00OR22725 with the US Department of Energy (DOE). The US government retains and the publisher, by accepting the article for publication, acknowledges that the US government retains a nonexclusive, paid-up, irrevocable, worldwide license to publish or reproduce the published form of this manuscript, or allow others to do so, for US government purposes. DOE will provide public access to these results of federally sponsored research in accordance with the DOE Public Access Plan (https://www.energy.gov/doe-public-access-plan).

Abstract: Solar photovoltaic (PV) generation technology stands out as a scalable and cost-effective solution to enable the transition towards decarbonization. However, PV solar output, beyond the daily solar irradiance variability and unavailability during nights, is very sensitive to weather events like hurricanes. Hurricanes nucleate massive amounts of clouds around their centers, shading hundreds of kilometers in their path reducing PV power output. This research proposes a spatiotemporal method, implemented in MATLAB coding, to estimate the shading effect of hurricanes over a wide distribution of PV solar plants connected to a high voltage power infrastructure called U.S.-Caribbean-South America super grid. The complete interconnection of the U.S., Caribbeans, and South America results in the lowest power valley levels, i.e., an overall percentual reduction in PV power output caused by hurricane shading. The simulations assess the impact of hurricanes in ten synthetic trajectories spanning from Texas to Florida. The Caribbeans would also experience lower power valleys with expanded interconnectivity schemes. U.S.-Caribbean-South America super grid reduces Caribbean variability from 37.8% to 8.9%, in the case-study. The proposed spatiotemporal method for PV power profile estimation is a valuable tool for future solar power generation expansion, transmission planning, and system design considering the impact of hurricanes.

Keywords: Hurricanes; power profile assessment; power variability; PV solar; renewables; spatiotemporal method.

Citation: To be added by editorial staff during production.

Academic Editor: Firstname Lastname

Received: date
Revised: date
Accepted: date
Published: date

1. Introduction

1.1. Background

Anthropogenic-induced climate change has been linked to increased magnitude of hurricanes and precipitation in the Atlantic and Gulf Coasts, Hawaii, and Puerto Rico [1]. The causes of the increasing number of major hurricanes in the North Atlantic are credited to both climate change (higher ocean heat, sea surface temperature and cloud cover moisture) and climatic variability (El Niño Southern Oscillation and the Atlantic Multidecadal Oscillation [1].

Regardless of the causes and underlying mechanisms, still under investigation from weather and atmospheric scientists, this research focus on the effects of hurricanes.

Hurricanes cause major impact on electrical grids, specifically on the large-scale PV solar power generation capacity. The overall systemic impact of hurricanes on large-scale PV capacity integrated in high voltage super grids is not very well understood yet.

1.2. Literature Review

This brief review on the technical literature explores primarily two multidisciplinary domains: the impact hurricanes shading on PV solar power profile and the grid integration facilitated by large-scale power interconnectivity schemes, namely, super grids. Notably, these domains are seldom investigated together in existing literature. Consequently, this concise review adopts a distinct approach to provide a clear understanding of the context within the current body of literature, addressing identified gaps to be covered in this research.

1.2.1. Hurricane shading on PV power

In 2020, Cole et al. estimated the shading impact of hurricanes on a PV power plant in the US by collecting spatial-temporal weather data of the National Solar Radiation Database and applying to a software tool called System Advisor Model (SAM) [2]. They observed a reduction of PV power to 18 to 60% during the hurricane. Their simulations are specific to estimation of Hurricane Ike (category 4) impact on an assumed 200 MW PV plant in Galveston, Texas, with fixed-tilt angle of 20 degrees, and azimuth orientation of 180 degrees [2]. Their data-driven estimation included the effect of hurricane winds in cooling the PV array, and supposedly improving energy-conversion performance. They observed 5 days hurricane impact with major decay around 72h of the passage of the hurricane eye and suggesting such period for specification of battery autonomy for critical loads [2].

In 2021, Ceferino et al. elaborated a stochastic modeling of solar irradiance during hurricanes. They compiled data from the revised Atlantic hurricane database (HURDAT2) of 22 historical hurricanes crossing the Caribbeans, the Gulf of Mexico and making landfall in South coast of the US. [3]. They proposed four different parametric models of solar decay of a PV solar power plant and demonstrated consistency of the best one in comparison with the power density obtained by Cole et al. in 2020 [2]. While the association of hurricanes and impact on wind power is direct due to the strong kinetic energy released in a hurricane, the association of hurricane shading and solar power is not much noticed. The literature about hurricane shading and PV solar is very scarce.

1.2.2. Super grids

The worldwide expansion of transmission systems is much critical as clean energy transitions progress. New transmission lines are needed to be added or refurbished by 2040 to support nations to achieve their targets for greenhouse emissions reduction by renewables [4]. Super grids are high voltage transmission interconnectivity schemes for GW-scale cross-border power trading among countries and territories [5]. Super grids have been in ongoing or recent construction in the Europe [6], Southeast Asian countries [7], interregional China [8],[9] and Euro-Asia interconnector [10]. Super grids have been proposed and investigated for interconnection of Europe-North America [11], Mongolia-Russia-Japan-South Korea-China [12], China-South Korea-Japan [13], Japan-Taiwan-Philippines [14], Australia-Indonesia-Singapore [15], U.S.-Caribbeans-South America [16], Latin America [17], interregional North America [18], and Africa [19].

Super grids find application and value proposition for example in situations where two or more intermittent renewable sources are complementary but distant from each other, the demand is not flexible and energy storage is poorly available. Also, super grids have been investigated for enhancement of energy security between nations.

1.3. Research Gaps and Motivation

Research gaps are observed in the interdisciplinary space between hurricane shading on PV plants and systemic impact on large-scale super grids. The research gaps can be summarized into three classes.

The first one is the need for a tool to assess the impact of hurricanes on a multitude of PV power plants. The estimation method proposed by Cole et al. in 2020 focused just on one PV plant [2]. For being case-specific, their findings cannot be extrapolated for several PV power plants, in different fixed-tilts, located at different distances from the hurricane trajectory, possibly not covered by the database. It also remains to be addressed the non-critical loads, represented by power customers who cannot afford power backup systems. Such case-specific limitations do not blur the merits of their findings, which are still very relevant for the validation of the order magnitude of the results of this research. However, such limitation is an important gap explored in this research.

The second gap is derived from Ceferino et al. [3]. One of the limitations of the Ceferino's model, similarly to Cole et al., is that it does not extend the analysis to large-scale renewable power grids. This limitation is addressed in this research with the increment of quantity and distribution of PV solar plants along the countries served by the proposed U.S.-Caribbean super grid with and without extension to South America.

The third gap is the assessment of hurricane shading impact on PV power variability in super-grids. Despite vast literature, to be best of authors knowledge, super grids have never been investigated with exclusive interdisciplinary focus on the impact of hurricane shading on PV solar power plants. This is relevant because PV solar is in accelerated ongoing expansion. This is the research gap is explored by this research.

1.4. Challenges

This research proposes a method for estimation of PV solar power profiles aggregated into a super grid with the impact of hurricane shading. This research analyses different options of large-scale interconnectivity schemes for the proposed U.S.-Caribbean-South America super grid. Large amount of PV capacity concentrated along the hurricane trajectory (such as in the US contiguous territory) causes high aggregated power valleys. In this research, power valley is the magnitude of drop of power profile of PV plants caused by hurricanes.

From the perspective of solar irradiance, major hurricanes attract to its center eye large amounts of clouds, barring the full penetration of clear sky solar energy to the Earth's surface. Given its size not rarely exceeding 500 km radius, it causes significant spatiotemporal shading along its track over PV solar power plants for extended period and coverage [3]

From the perspective of power grid integration, the current endeavor to expedite the deployment of renewables in the energy transition away from fossil fuel, is pushing for a much-needed large scale interconnection of local high voltage power grids. According to the IEA, transmission lines length needs to be double in the U.S. and expanded 2.4 times worldwide, from the 2021 status until 2050 in the announced pledges scenario [4] for renewables expansion. Power transmission lines not just allow the efficient power flow from renewable power generation to consumers, but also supports the balancing of supply-demand power transactions, by cutting the intermittent renewables power peak in one geographical location to fill the power valley in other sections of the integrated power grid [20]. However, overhead aerial transmission lines are extremely vulnerable to hurricane wind forces [21] and aesthetics of towers and lines are perceived as having a negative influence on the landscape by land property owners and residents [22]. Given this challenging context, power transmission based on submarine subsea cables, which is inherently resilient to hurricanes and immune to land property compensation or blockade, demonstrates a value proposition to support fast and mass deployment of intermittent renewables [16]. The main challenge of this research is to envision a realistic scenario with renewables PV, propose and implement an innovated method for PV power estimation under hurricanes, and deliver a tool to bridge the interdisciplinary gap between

extreme weather science and electrical power system with real world application for super grid transmission systems planning, design and large-scale power systems simulations.

1.5. Contribution

This research investigates the impact of hurricane shading on PV solar power plants within a U.S.-Caribbean-South America super grid topology. Originally proposed for interconnecting wind power plants in [16], this super grid addresses the challenge of reducing power variability during extreme weather events. The study makes significant contributions by proposing a novel spatiotemporal method for estimating PV power profiles under hurricanes, filling gaps in the literature. Simulation results demonstrate reduced PV power variability when the Caribbean super grid is connected to the US or South America. This comprehensive and versatile method proves essential for future transmission systems planning, design, and power flow simulations of renewables under extreme weather conditions. The research explores different interconnectivity schemes, emphasizing the benefits of the U.S.-Caribbean-South America super grid. The study paves the way for future investigations into feasibility, cost-benefit analysis, and power estimation under non-hurricane conditions across the super grid.

1.6. Paper Organization

This work is organized as follow: Section 2 proposes a spatiotemporal method to quantify the magnitude of hurricane shading impact on PV solar power plants. Section 3 presents simulation results using the proposed method and a comparative analysis of power profile variability under different scenarios. Section 4 presents an analysis of consistency of the method. Section 5 concludes the work discussing scope restrictions, merits, limitations, and future work.

2. Materials and Methods

The materials on this research include specific technical publications that played a critical role in establishing the input parameters for the modeling and simulation process.

The proposed spatiotemporal method for estimating PV solar power profile in super grids under hurricane shading integrates models and outlines a potential expansion of PV solar capacity as a case scenario. The method was implemented in MATLAB coding to model the components of the algorithm and generate the simulation results. The proposed method integrates the following components:

- Model of global irradiance on the tilted PV module [23], formulated in Appendix A.
- Model of irradiance decay by hurricanes shading effect [3].
- Conversion of irradiance on PV module into power profile, as formulated in [24].
- Model of the hurricane movement over a synthetic parabolic trajectory.
- Model of future PV solar capacity expansion along U.S.-Caribbean-South America super grid.
- Spatiotemporal estimation of PV solar power profile of super grids under hurricane shading.

2.1. Model of Global irradiance on the tilted PV module

Global irradiance on the tilted PV module is a model for estimation of solar radiation peak power (kW/m^2) and energy (kWh/m^2) in any given latitude and day of the year. By selecting a specification of PV module technology, quantity, size of the PV cell, tilt angle and azimuth orientation, the model also generates the power profile from the PV solar plant. The details and the equations of the global irradiance model in [23] are described in the Appendix A.

The model is used to generate solar irradiance profiles of each PV plant for 14 days period. The coordinates of the PV plants are inputs for the estimation of solar irradiance.

2.2. *Model of the hurricane shading effect*

In 2021, Ceferino et al. elaborated the modeling of irradiance decay during hurricanes in function of the certain parameters. **Table 1** also shows such parameters, its values and descriptions, and the sources of literature.

Table 1. Parameters of hurricanes and shading.

Parameters	Description	Michael (2018)	Charley (2004)	Wilma (2005)	Sources
C	hurricane category	5	4	3	[20]
a_1	slope factor	1.97	1.97	1.97	[3]
a_2	slope factor	0.0965	0.0965	0.0965	[3]
b_1	short-distance correction factor	1.15	1.15	1.15	[3]
b_2	short-distance correction factor	-0.126	-0.126	-0.126	[3]
c_1	scale factor	2.48	2.48	2.48	[3]
c_2	scale factor	-0.139	-0.139	-0.139	[3]
$ROCI$ for onshore	radii of the outermost closed isobar	150 nautical miles (278 km)	100 nautical miles (185 km)	250 nautical miles (463 km)	NOAA [25 - 27]
$ROCI$ for offshore	radii of the outermost closed isobar	200 nautical miles (370 km)	100 nautical miles (185 km)	300 nautical miles (556 km)	NOAA [25 -27]
d, R, and f	absolute distance from hurricane eye, relative distance from hurricane eye, and functional form	recalculated after each step	recalculated after each step	recalculated after each step	[3]
Δt_h	simulation time step	1 h	1 h	1 h	[20]
V_{tr}	hurricane translational speed	9.722 m/s	12.5 m/s	13.333 m/s	[20]

From data obtained from the US National Oceanic and Atmospheric Administration (NOAA), the radii of the outermost closed isobar (ROCI) value is not directly proportional to the hurricane category [25-27]. It is important to note that ROCI is associated to the extent of shading of solar irradiance, as observed in [3]. Table 1 shows a category-4 hurricane Charley (2004) with smaller ROCI value than category-5 hurricane Michael (2018) and category-3 hurricane Wilma (2005). The data from NOAA implies that not always a high category hurricane produces more shading than a low category hurricane.

This research makes use of parameter-based equations elaborated by Ceferino et al. to represent the shading effect of hurricanes on a PV solar plant. The parametric equation proposed, and validated by Ceferino et al., in 2021, is as follows [3]:

$$I^h = I \times e^{f(R,C)} \quad (1)$$

$$f(R,C) = \begin{cases} (a_2C + a_1) \times ln\left(\frac{R+(b_2C+b_1)}{c_2C+c_1}\right) & , \; if \; R + (b_2C + b_1) < (c_2C + c_1) \\ 0 & , \; if \; R + (b_2C + b_1) \geq (c_2C + c_1) \end{cases} \quad (2)$$

$$R = d/ROCI \quad (3)$$

where I^h is clearness factor during a hurricane, and I is made equal to the unity in this research, for per-unit calculation. The remaining parameters are described in Table 1.

Figure 1 shows the implementation of the hurricane exponential clearness factor implemented in MATLAB coding and based on the parametric equations (1), (2), and (3) for the parameters of hurricane Wilma (2005) with onshore $ROCI$ of 463 km, shown in **Table 2**. There are two clearness factor curves because the $ROCI$ of hurricane in onshore trajectory may be slightly different from offshore, according to the hurricanes data tracked by NOAA [25-27]. The shading effect radii (600 and 720 km in **Figure 1** extends beyond the $ROCI$ radius of 463 km and 556 km for onshore and offshore conditions, respectively. This overextension of shading corroborates the findings of Ceferino et al., which also observed decay extending to approximately 1.3 x $ROCI$ [3].

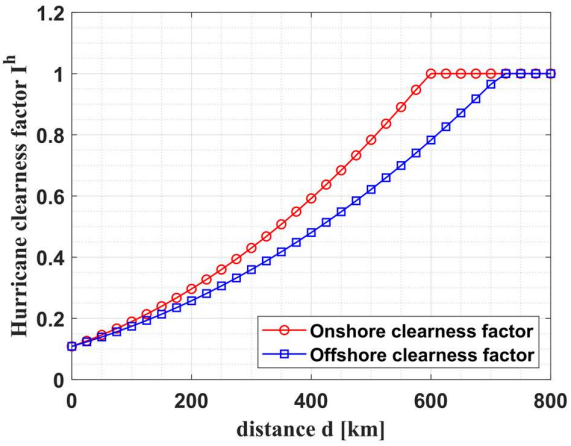

Figure 1. Exponential clearness factor I^h versus distance d.

The hurricane shading effect values less than the unity means that the irradiance absorbed by the PV cells is partially blocked by the hurricane clouds, reducing its power generation in proximity to the hurricane center. In this model, hurricane's clouds do not shade PV power plants located more than 600 km and 720 km away from its eye over onshore and offshore locations, respectively.

2.3. Conversion of solar energy into alternating current electric power.

Table 2 shows the PV cell data and environmental parameters for the conversion of solar irradiation into PV solar power profile.

Table 2. PV cell data and environmental parameters.

Parameters	Specification and environment variables	Sources
PV module technology	monocrystalline	[3]
Tilt type	Fixed open rack (hurricane resistant)	[3]
Tilt angle	Made equal to plant latitude (degrees)	[3]
Azimuth orientation	180 degrees (North hemisphere) 0 degrees (South hemisphere)	[3]
$P_{PV,rated}$	PV rated ac power output	Appendix-B

Hurricane clouds shading reduces the total solar irradiation absorbed by the PV plants by the clearness factor during hurricane $I^h(t)$. This research assumes that the PV plants have power capacity values ($P_{PV,rated}$) referred to alternating current output and are adequately sized to absorb the full peak irradiance on the PV solar plant on Sept 15th at noon. This date is conveniently selected in the middle of the US hurricanes season, from June 1st to Nov 30. The instantaneous power in each PV plant is calculated by [3]:

$$P_{PV}(t) = P_{PV,rated} \cdot I^h(t) \,.\, G_{T,\beta}(t) \quad (4)$$

where: $P_{PV}(t)$ is the instantaneous power profile of each PV plant, $P_{PV,rated}$ is power capacity referred to alternating current output, I^h is the clearness factor, and $G_{T,\beta}$ is total solar irradiation absorbed by fixed tilted PV module.

2.4. Model of the hurricane movement over a synthetic parabolic trajectory.

This subsection describes the first major piece of contribution of this research: a synthesis of hurricane trajectories.

Historical hurricanes, tracked by NOAA [25-27] leave a trail of likely trajectories, forming a corridor of hurricanes. This corridor covers vast portions of the Caribbean Sea, Gulf of Mexico, and contiguous U.S. territory. Aiming at being comprehensive enough to obtain the worst-case scenario of PV power drop on a PV solar plant from hurricanes in all positions inside the corridor, this research modeled the hurricane movement over a band of ten parabola-shape trajectories covering the entire observed corridor. The reasoning for pursuing the worst-case scenario is that a power grid status should be maintained at high levels of operational continuity and resilience even in extreme weather conditions. This research does not simulate a hurricane over a specific historical trajectory because there is not guarantee that it is the worst-case scenario, and that a future hurricane would exactly pass over a same specific historical trajectory. Also, the approximation of hurricane trajectories by parabolas has been traditionally proposed in the existing literature [16][20].

The equations for parabola-shaped trajectories for hurricanes representation are [20]:

$$y = a_3 x^2 + b_3 x + c_3 \quad (5)$$

where: y is longitude, x is latitude of the eye of the hurricane, and a_3, b_3 , and c_3 are the parabola's coefficients.

The North Atlantic hurricanes corridor changes the direction with vertex at latitude x of 30º degrees and longitude y from Texas to offshore Florida, as observed on the NOAA's hurricane tracking system [NOAA et al]. Assuming ten equidistant parabola vertex points (x_{vertex}, y_{vertex}) in such segment, coefficients b_3 , a_3 and c_3 for each parabola trajectory can be calculated by [20]:

$$b_3 = -2a_3 . x_{vertex} \quad (6)$$

$$a_3 = \frac{x - x_{vertex}}{y - y_{vertex}} \quad (7)$$

$$c_3 = y - a_3 x^2 - b_3 x \quad (8)$$

where: y is longitude, x is latitude of the eye of the hurricane, x_{vertex} is the latitude vertex of the parabola, and y_{vertex} is the longitude vertex of the parabola.

From ten equidistant parabola origin points (x_{origin}, y_{origin}) covering the hurricanes corridor in NOAA hurricane tracking map [28], the latitude and longitude of the synthetic parabolic trajectory (x_{k+1} , y_{k+1}) is calculated by [20]:

$$x_{k+1} = x_k + \Delta Step.sin\theta \quad (9)$$

$$y_{k+1} = a_3 {x_{k+1}}^2 + b_3 x_{k+1} + c_3 \quad (10)$$

where $\Delta Step$ is the angle step of 1-hour hurricane movement over the surface of the Earth, and angle θ is [20]:

$$\theta = \frac{\pi}{2} - \arctan\left(2a_3.x_k + b_3\right) \quad (11)$$

where: a_3 and b_3 are parabola coefficients, and x_k is the latitude of hurricane eye in each step.

Table 3 shows the input coordinates for the synthetic modeling of hurricane trajectory as parabola, taking into consideration the hurricane's corridor formed by historical trajectories tracked by NOAA [28].

Table 3. Origin and vertex points of parabola for hurricane trajectory modeling.

Track #	x_{origin} [°]	y_{origin} [°]	x_{vertex} [°]	y_{vertex} [°]
1	7	-69.9563	30	-100.0
2	8	-70.2564	30	-97.7778
3	9	-33.1111	30	-95.5556
4	10	-33.1667	30	-93.3333
5	11	-33.2222	30	-91.1111
6	12	-33.2778	30	-88.8889
7	13	-33.3333	30	-86.6667
8	14	-33.3889	30	-84.4444
9	15	-33.4444	30	-82.2222
10	16	-33.5	30	-80

Figure 2 shows the synthetic parabolic trajectories of hurricanes. This multicolor band of ten parabolic trajectories covers most of the historical hurricane's trajectories tracked by the National Hurricane Center [28]. This band of trajectories aims at encompassing the hurricane's corridor. Any future hurricane trajectory is expected to be a combination of two or more synthetic trajectories within the hurricane's corridor.

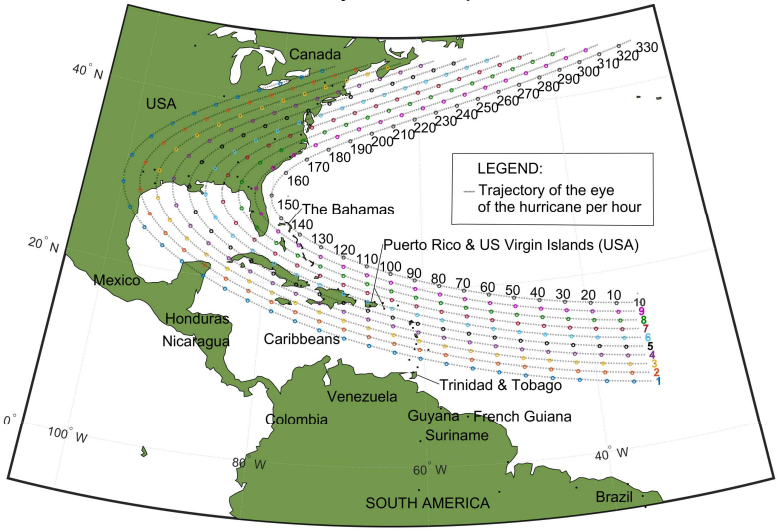

Figure 2: Synthetic parabolic trajectories of hurricane, adapted from [16].

The band of parabolic trajectories show in **Figure 2** cover all US southern states between Texas and Florida, all countries, and territories in the Caribbeans. Also, hurricanes in latitude lower than trajectory #1 are very rare, according to NOAA repository of historical hurricanes trajectories [28].

2.5. Model of future PV solar capacity expansion in US, Caribbean and South America

This subsection describes the second major piece of contribution of this research: a scenario of future PV solar capacity expansion based on a compilation of demographic data and existing fossil fuel power capacity to be gradually displaced by renewables.

Table 4 shows some of those data supporting a possible scenario of renewable PV solar power capacity. This research assumes a scenario that future PV power capacity (P_{PVcap}) would substitute half ($F_e = 50\%$) of the fossil dependence:

$$P_{PVcap} = P_{total} \times F_d \times F_e \quad (12)$$

where P_{total} is the total power capacity (including fossil) of the country or territory, F_d is the fossil dependence, and F_e is the PV expansion factor.

This PV sharing factor of 50% is an assumption of this research considering that the other 50% is assumed to be supplied by other renewable energy sources, such as wind power in the future.

The actual commitment and execution of each country and territories in the Americas and Caribbeans for the expansion of PV solar carries innumerous uncertainties. Some uncertainties are not predictable, e.g., the willingness of government officials to keep supporting strategic plans for renewables. Due to lack of available data, the PV solar power capacity of Anguilla in 2050 (8 MW), by proportionality of its population, was assumed to be half of the British Virgins Islands (16 MW). The error associated to this PV capacity estimate of Anguilla is not representative in face of the total PV power capacity encompassed by this simulation (1,072,283 MW).

Despite uncertainties, a cumulative PV sharing factor of 50% of PV solar over total existing power capacity does not lead to an overestimation of results since the total existing power capacity is a realistic reference cap, also assumed to be adequately supplying an existing power demand. This work is assuming that none of the small countries and territories in **Table 4** will become a major exporter of PV solar power, i.e., with renewable capacity far exceeding its previous local total power capacity and demand. The primary function of the U.S.-Caribbean-South America SG is to smooth power variability by instantaneous spatiotemporal power support of islands experiencing power valley or peaks caused by extreme weather events. Some previous targets for renewables expansion in these Caribbean countries in general shows modest numbers: Antigua and Barbuda (15% by 2030), Bahamas (30% by 2030), Barbados (29% by 2029), Belize (50% by no specific date), Cuba (24% by 2030), Dominica (100% by no specific date), Dominican Republic (20% by 2016), Grenada (20% by 2020), Guyana (90% by no specific date), Haiti (50% by 2020), Jamaica (30% by 2020), St Kitts and Nevis (20% by 2015), St Lucia (35% by 2020), St Vincent and the Grenadines (60% by 2020), Trinidad and Tobago (100 MW of wind by not specific date and no specific share for PV solar) [29].

This work simulates the impact of hurricane shading in 2050 on PV solar generation sized to cover 50% of the total existing power capacity (including fossil power) in case of small islands or territories without publicly available official government target for PV expansion.

Table 4. Demographics and fossil fuel dependence in US, Caribbeans and South America.

Countries or territories	Population	Total capacity [MW]	Fossil dep. (F_d)	2050 Cumulative PV [MWac]	PV latitude, and longitude [°]	Ref.
USA	339,665,118	1,143,266 (est. 2020)	59.9%	1,000,000	Appendix B	[30-31]
The Bahamas	358,508	578	99.8%	288	24.698981, -77.789604	[30]
Cuba	10,985,974	7,479	95.5%	3,571	21.598426, -78.974099; 19.907734, -75.218468; 20.358009, -74.504742	[30]
Haiti	11,470,261	3,453	85.8%	1,481	18.576618, -72.296021	[30]
Jamaica	2,820,982	1,216	87.5%	532	17.876148, -76.582014	[30]
Dominican Republic	10,790,744	5,674	93.4%	2,650	19.755237, -70.564617; 19.267622, -69.730425; 18.568692, -68.348547	[30]
Puerto Rico	3,057,311	6,180	94.8%	2,929	18.494859, -67.135248; 18.010464, -66.563032; 18.436395, -66.002171	[30]
Virgin Islands (US)	104,917	321	98.9%	159	17.699028, -64.797495	[30]
British Virgin Islands	39,369	33	98.8%	16	18.339107, -64.966938	[30]
Anguilla	19,079	16	98.8%	8	18.043635, -63.113343	[30]
Guadeloupe	390,704	551	68.9%	190	16.269481, -61.526794	[32-33]
Dominica	74,656	42	74.8%	16	15.545482, -61.300085	[30]
Martinique	371,246	438	85.1%	186	14.595778, -61.000148	[32-33]
St Lucia	167,591	92	99.1%	46	13.736792, -60.949993	[30]
St Vincent and Grenadines	100,804	49	73.5%	18	13.163664, -61.151563	[30]
Grenada	114,299	55	98.3%	27	12.007409, -61.785788	[30]
Barbados	303,431	311	95.9%	149	13.080299, -59.488530	[30]
Trinidad & Tobago	1,407,460	2,123	99.9%	1,060	10.601978, -61.339610; 11.152808, -60.839655	[30]
Guyana	791,739	380	97.4%	185	6.504099, -58.252893	[30]
Suriname	639,759	542	40.5%	220	5.456538, -55.199946	[30]
French Guiana	301,099	281	37%	52	4.822596, -52.364161	[34]
Brazil	218,689,757	195,037	11.8%	58,500	Appendix B	[30], [35]
Total	602,392,300	1,368,117	-	1,072,283	-	-

The basis for estimation of the projected utility-scale PV solar power capacity of the U.S. and Brazil in 2050, being 98.7% of the PV capacity interconnected by the U.S.-Caribbean-South America SG, was obtained from studies and plans elaborated by US National Laboratories for the DOE and the Brazilian Energy Research Company [31], [35]. The projected 2050 PV capacity of the U.S. and Brazil is detailed separately in Appendix B.

Figure 3 shows the U.S.-Caribbean-South America super grid originally proposed by Itiki et al in 2023 to support the expansion of wind power [16]. Over the same super grid topology, this research also proposes a physical distribution of PV power capacity in the U.S., Caribbeans and South America.

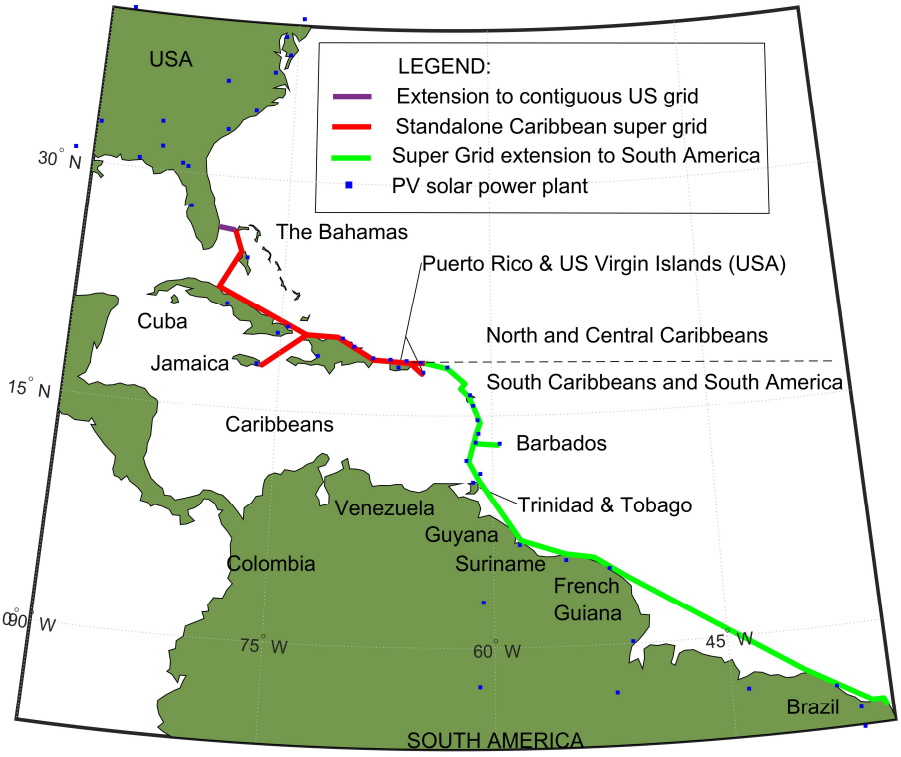

Figure 3. Proposed expansion of the U.S.-Caribbean-South America super grid in 2050, adapted for PV power from [16].

The purpose of the original proposal of the U.S.-Caribbean-South America super grid is to provide a comprehensive power grid infrastructure for massive expansion of wind power capacity in the region [16]. This super grid infrastructure can smooth the percentual power variability caused by intermittent renewable energy sources, particularly during hurricanes [16]. In contrast, the focus of this research is exclusively on PV power variability generated by hurricanes in the super grid.

For purpose of simulations, this research assumes that this proposed U.S.-Caribbean-South America super grid would be operationally ready in 2050. The projection of 2050 PV capacity expansion in the US and Brazil is consolidated based on existing plans and studies [31], [35].

In the United States, a comprehensive plan for expansion of solar power capacity was elaborated by the National Renewable Energy Laboratory (NREL) in 2021 [31]. Three scenarios of solar power capacity were projected for 2050 US: (a) Decarb+E scenario with 1,600 GW, (b) Decarb scenario with 1,000 GW, and (c) Reference scenario with 600 GW. In 2022, the PV capacity in the US was around 109 GW, according to Appendix A. For simulation purposes, this work adopts the Decarb scenario with 1,000 GW in 2050, which is the mean-average scenario. The US PV capacity values shown on Appendix B is multiplied by 9.17 times for the simulations of future 2050 scenario of 1,000 GW in the U.S.

In Brazil, the Brazilian Energy Research Company, a Brazilian federal-owned organization, issued the National Energy Plan 2050 (PNE). The centralized PV generation capacity (excluding residential or commercial PV) is estimated to reach between 27 to 90 GW in 2050 [35]. In 2022, the centralized PV generation capacity in Brazil was around 18.13 GW, according to Appendix A. For simulation purposes, this work adopts the mean-average scenario of 58.5 GW in 2050. The Brazilian PV capacity values shown on Appendix B are multiplied by 3.23 times for the simulations of the future 2050 scenario of 58.5 GW in Brazil.

This research assumes, as simulation scenario, that a proposed U.S.-Caribbean-South America super grid does not restrain in 2050 the cross-country high voltage power trading and operations in the US, Caribbeans and South American region.

2.6. Proposed spatiotemporal algorithm for estimation of PV solar power under hurricanes shading.

The proposed algorithm processes all modeling described in previous subsections and generates an estimated aggregated power profile from all PV solar plants. **Figure 4** shows such proposed algorithm for estimation of PV power under hurricanes shading.

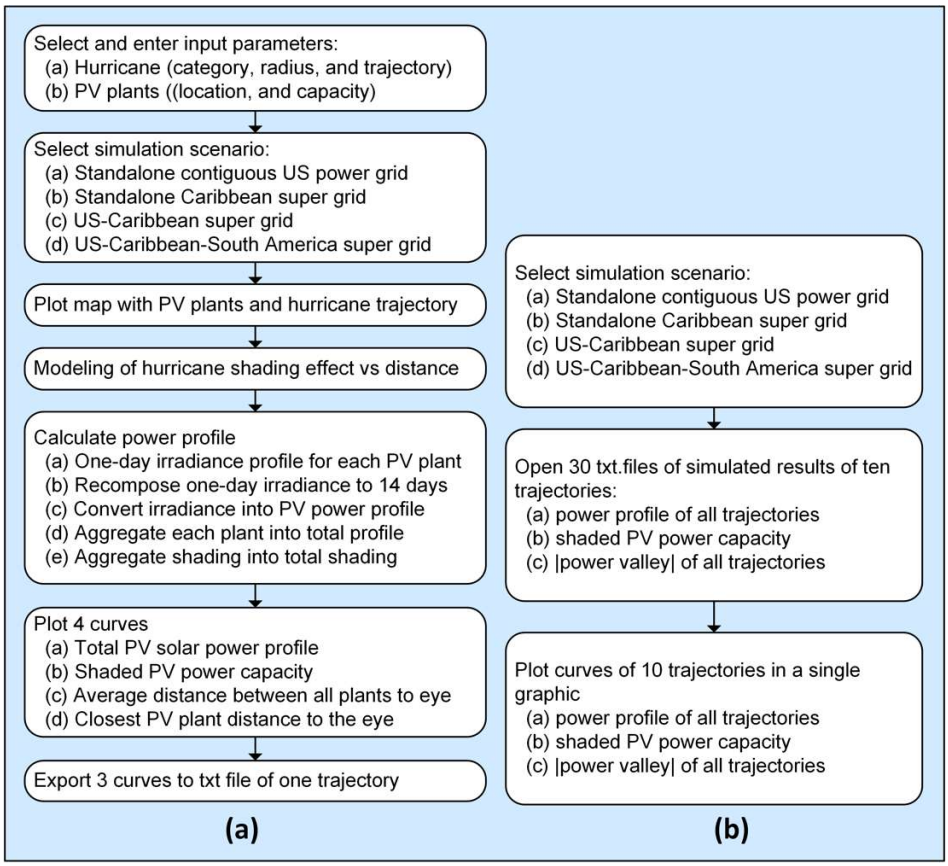

Figure 4. Algorithm for estimation of PV solar power under hurricanes over: (a) a single trajectory, (b) ten trajectories.

The algorithm was initially developed to estimate PV power profile under a hurricane in a single parabolic trajectory as shown in **Figure 4**(a). The purpose was to analyze the evolution of PV power profile while a hurricane crosses the Caribbean islands and make landfall in the contiguous US. This algorithm is used to investigate trajectory #7, shown in **Figure 2**, because of proximity to large density of PV solar plants in the Caribbeans and in the US, and the combination of four simulation scenarios of super grid connectivity. **Figure 4**(a) has 7 blocks: Block 1 receives the input parameters of the selected hurricane (e.g., radius), the PV solar plants characterization (e.g., location and power capacity). In block 2, the user selects the interconnectivity scheme. Block 3 plots the input data on a map to visually characterize the simulation scenario, PV plant's locations, and the selected hurricane trajectory. Block 4 implements the modeling of the hurricane shading in function of the distance according to equations (1), (2) and (3). Block 5 integrates several steps: the modeling of the clear sky irradiance over each PV plant in pre-hurricane conditions for 14 days, modeling of the translational movement of the hurricane over a

parabola trajectory for 14 days period, calculation of the distance between each PV plant to the hurricane eye, the application of the hurricane shading effect based on the distance of plant to the eye, and the conversion of shaded irradiance into PV power profile in each plant based on its rated capacity. Block 6 delivers the plotting of four curves, leading the final estimation of PV power profile under hurricanes. Block 7 exports the simulation curves "Total PV solar power profile", "Shaded PV power capacity", and "Average distance of all plants to the eye", in text format.

With the necessity of empowering the method with generic capability and coverage of the entire hurricane's corridor, not just an individual and specific trajectory #7, the algorithm was complemented with another set of blocks shown in **Figure 4**(b). The comparative analysis of PV power profile in ten trajectories allows visual identification of the trajectory causing the deepest power valley in each connectivity scheme. Since the hurricane trajectory cannot be diverted by humans, the power grid resilience must be designed, in principle, to withstand the worst-case trajectory and mitigating the deepest power valley. One of the possible solutions to smooth power valleys is proposed in this research with large-scale interconnectivity schemes by super grids. Even disregarding super grids as a solution to reduce power variability for whatever reasons, the proposed method to estimate the profile depth of power valley is still an important parameter for the sizing of the capacity of the energy storage systems (battery, or even pumped hydro) to fill the valley. The extended blocks shown in **Figure 4**(b) aims at supporting such assessment and future design.

2.7. Assumptions

This research assumes that the PV solar power plant integrity would not be damaged by high winds of hurricanes by the time this proposed U.S.-Caribbean-South America super grid becomes a physically constructed reality in the next tens of couples of years ahead. This assumption is reasonable because a PV power plant damaged by recurrent impact of hurricanes would be upgraded with hurricane-proof PV modules or an equivalent protection device to keep economic feasibility.

This research also assumes that batteries are not affordable in short term and in mass scale to most of the impoverished islands of the Caribbeans. This research disregards the large-scale power retrieval from batteries.

The simulation scenarios are projected for the year 2050, assuming a massive deployment of PV solar capacity in the US, Caribbeans, and South America. Also, it is assumed that the proposed Caribbean super grid, in its variants of interconnectivity schemes, would be ready for operation in 2050, overcoming the phases of regulatory approval, international agreements with involved countries, engineering, procurement, construction, commissioning, and final approval for operation.

Since the focus of this research is the exclusive impact of hurricanes on PV shading and power valley, the pre-hurricane conditions are assumed to be in clear sky conditions. This assumption aims at eliminating uncertainties about weather conditions in pre-hurricane conditions. This method is not focused on reproducing historical hurricanes or estimating weather systems in 2050 based on probabilistic average clearness conditions in 2023. In other words, this work does not propose to incorporate projections about climate change, weather, and ambient variables, in 2050.

The daily solar irradiance profile over the PV plant is assumed to be the same in the first and the last 10th day of the hurricane simulation. Ten consecutive days is not considered long enough to cause seasonal irradiance variability. Instead, the 14 days hurricane shading dynamics is assumed to carry more significant impact on the PV power generation. This research disregards shading due to topography (mountains) or other obstructions (trees and tall buildings). Future studies may also address this topic.

3. Results

The simulations were carried out on four scenarios of power grid topology impacted by a hurricane over trajectory #7:

- Standalone contiguous US power grid
- Standalone Caribbean super grid
- U.S.-Caribbean super grid
- U.S.-Caribbean-South America super grid

Also, it was simulated two scenarios with hurricanes in all ten synthetic trajectories over the U.S.-Caribbean-South America super grid, and over the standalone Caribbean super grid.

Figure 5 shows the geospatial scenario with a category-3 hurricane over synthetic parabolic trajectory # 7 impacting the PV solar plants on the U.S.-Caribbean-South America super grid. The trajectory of the hurricane eye is marked every 10 hours until 330 hours (approximately 14 days). The PV plants under consideration are those indicated in **Table 4** and Appendix B.

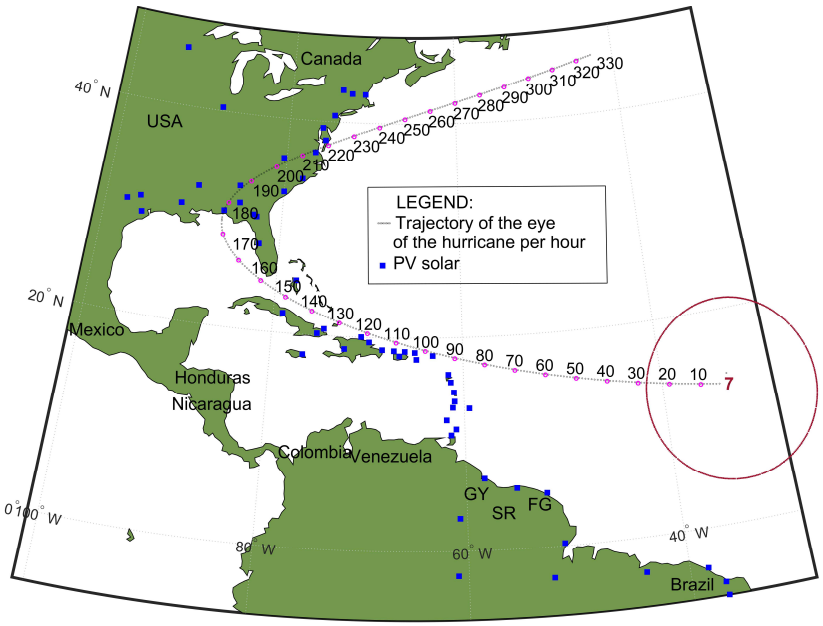

Figure 5. Hurricane over trajectory #7 passing through PV plants of the U.S.-Caribbean-South America super grid.

In the scenario of Standalone contiguous US power grid, the hurricane impacts only 36 PV solar plants. The PV plants in the Caribbeans and South America are not interconnected and aggregated in this scenario.

In the scenario of Standalone Caribbean super grid, the hurricane impacts 14 turbines in the northern part of the Caribbean islands. The PV plants in the contiguous U.S. grid and South Caribbean and South America are not interconnected and aggregated in this scenario.

In the scenario of U.S.-Caribbean super grid, 50 PV solar plants are interconnected and aggregated in super grid.

In the scenario of U.S.-Caribbean-South America super grid, the simulations cover all 90 PV plants, most of them shown on **Figure 5**, and some others in the US West Coast states, and Brazil's southern states, as indicated in Appendix B.

3.1. Standalone contiguous US power grid

In this scenario, the simulation covers the impact of hurricane on PV solar power plants on the contiguous US power grid. It excludes Hawaii, Alaska, and US Caribbean territories of Puerto Rico and US Virgins Islands. It is assumed that in 2050, Texas power grid is operating interconnected with the contiguous US power grid. In this scenario, there is no Caribbean super grid and any interconnection of it with the US and South America.

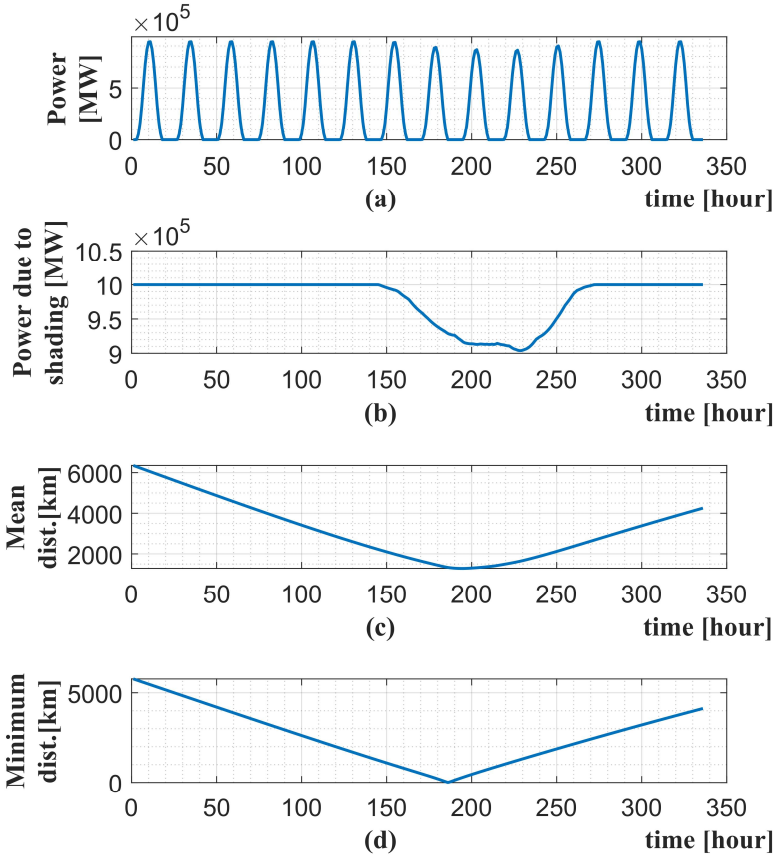

Figure 6. Hurricane over trajectory #7 passing through PV plants in standalone US contiguous power grid.

Figure 6(a) shows the total PV power profile generated by the PV power plants on the contiguous US power grid under the spatiotemporal impact of hurricane shading. The impact of the hurricane depends on the time in which it approaches to the PV solar power plant. The impact of hurricane shading on PV solar power profile is higher during the day period. There is not power dropping impact from hurricane shading on PV solar during the night period.

Figure 6(b) shows the shading effect during the passage of the hurricane in Florida and the US East Coast. The power valley represents the local shading on the PV solar plants due to proximity of hurricane clouds. This profile is decoupled from the variable radiance of the sun to show the exclusive impact of the hurricane shading on the aggregate PV plant capacity.

Figure 6(c) shows the mean geometric distance of all PV solar plants to the hurricane eye. This curve indicates how close the PV solar plants are in average to the hurricane. The lower the distance, the greater the magnitude of power valleys on **Figure 6**(b), and more modest the total PV solar power profile on **Figure 6**(a).

Figure 6(d) shows one of the PV solar plants with the closest distance from the hurricane eye. The continuous tracking of each hurricane is necessary because the shading effect depends on the distance between the hurricane eye and each PV solar plants. In this case, the hurricane almost touches the PV power plant in West Florida at time 185h as observed on **Figure 5**, corroborating the observation of minimum distance in **Figure 6**(d) at the same time.

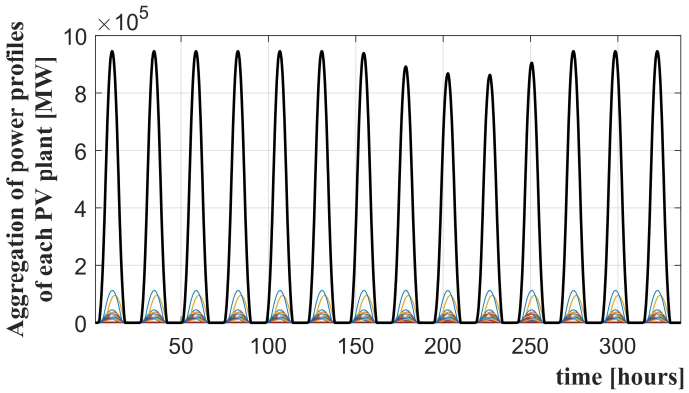

Figure 7. Aggregation of power profiles of each PV solar power plant in the standalone US contiguous power grid.

Figure 7 shows the individual power profiles of PV solar plants in the contiguous US. **Figure 7** also shows in black color the aggregated power profile of all PV solar plants, connected to the US contiguous power grid.

Figure 8 shows the per unit normalized power in each PV solar plant. Shading of the hurricane causes a spatiotemporal capacity reduction on each PV solar plant. The values are normalized to the unit reference to show the relative impact of the hurricane shading on each PV solar power plant. The shading effect on the clearness index intensifies while the hurricane is moving between time 150 to 265h, over Florida and the US East coast. This temporal effect matches the translational movement of the hurricane eye shown in **Figure 5**.

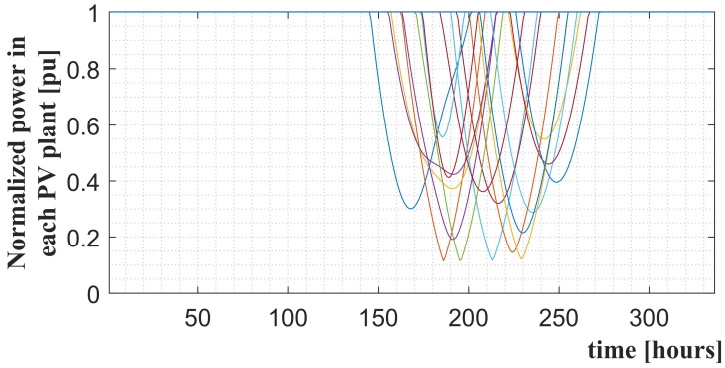

Figure 8. Normalized power in each PV solar power plant in the standalone US contiguous power grid.

Notably in **Figure 8**, four PV plants experience an equivalent capacity reduction up to 88% of their rated values during two days of hurricane shading. For the purposes of this research, it is assumed that these PV plants are all grid-connected. However, setting aside the consideration of grid-connectivity and assuming each PV plant functions as a microgrid without external grid connection, a hurricane-induced power valley of up to 88% for two days holds significant implications for the design of the energy storage system backing up the power shortage. Super grids, on the other hand, effectively mitigate such percentual power variability, and the assessment of this reduction is investigated in the simulations.

3.2. Standalone Caribbean super grid

In this scenario, the simulation covers the impact of hurricane on PV solar power plants on the standalone Caribbean super grid, including the US territories of Puerto Rico and US Virgin Islands. It excludes the contiguous US, and southern islands of the Caribbeans. It is assumed that in 2050, the Caribbean super grid is operationally ready but without any interconnection with the US, South Caribbeans and South America.

Figure 9(a) shows the total PV power profile generated by the PV power plants on the standalone Caribbean super grid under the spatiotemporal impact of hurricane shading.

Figure 9(b) shows the shading effect during the passage of the hurricane over US Virgin Islands, Puerto Rico, Dominican Republic, Haiti, Cuba, and The Bahamas, i.e., the North and Central Caribbeans. The local shading on the PV solar plants occurs between time 85 h and 170 h while the hurricane is passing through such islands.

Figure 9(c) shows the mean geometric distance of all PV solar plants to the hurricane eye. This curve indicates how close the PV solar plants are in average to the hurricane. The lower the distance, the greater the magnitude of power valleys on **Figure 9**(b). After time 180 h, the hurricane parabolic trajectory reaches its negative longitudinal apex. After the hurricane turning eastward, its mean average distance to the PV plants sustains 2,000 km distance. However, this distance is outside the hurricane shading and does not produce power valley after time 170 h.

Figure 9(d) shows the PV power plant in British Virgin Islands with the closest distance from the hurricane eye at time 105 h.

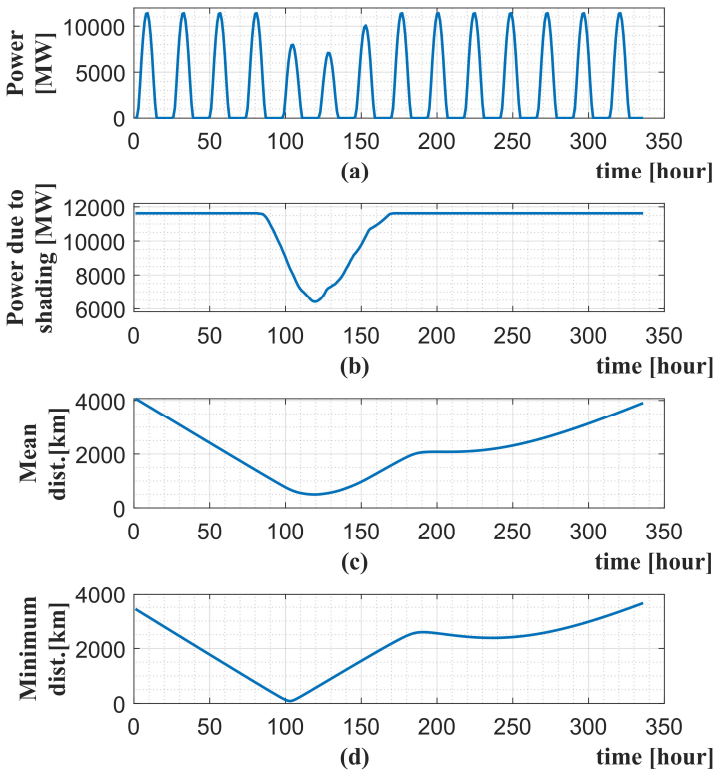

Figure 9. Hurricane over trajectory #7 passing through PV plants of the standalone Caribbean super grid.

Figure 10 shows the individual power profiles of the PV solar plants in the standalone Caribbean super grid. The black color curve is the aggregated power profile of all PV solar plants, i.e., the same profile shown on **Figure 9**(a).

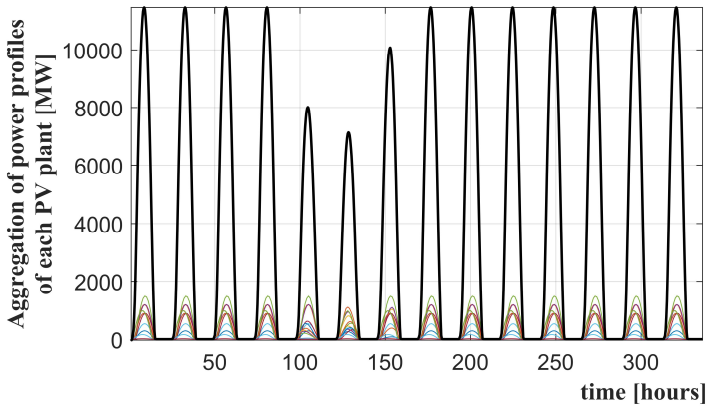

Figure 10. Aggregation of power profiles of each PV solar power plant in the standalone Caribbean super grid.

3.3. U.S.-Caribbean super grid

In this scenario, the simulation covers the impact of hurricane on PV solar power plants with the contiguous U.S. power grid is interconnected to the Caribbean super grid. This scenario is thus called U.S.-Caribbean super grid and requires a submarine power interconnector between Florida and The Bahamas and the extension of the grid until the

U.S. overseas territories of Puerto Rico and U.S. Virgin Islands. The purpose of this scenario is to assess the potential benefit of large-scale integration of standalone power grids in reducing the overall spatiotemporal power variability.

Figure11(a) shows the total power profile generated by the PV power plants of the U.S.-Caribbean-South America super grid under the spatiotemporal impact of hurricane shading. The impact of the hurricane is observed between time 160 h and 260 h.

Figure 11(b) shows the reduction of PV power capacity due to hurricane shading effect between time 160 h and 260 h. The power valley from the hurricane over the Caribbeans is relatively negligible as compared Florida and the U.S. East coast because the power capacity in the U.S. East coast is more robust than in the Caribbeans.

Figure 11(c) shows the mean geometric distance of all PV solar plants to the hurricane eye. This curve indicates how close in average the PV solar plants are to the hurricane.

Figure 11(d) shows the PV solar plant in West Florida with the closest distance from the hurricane eye at time 189 h.

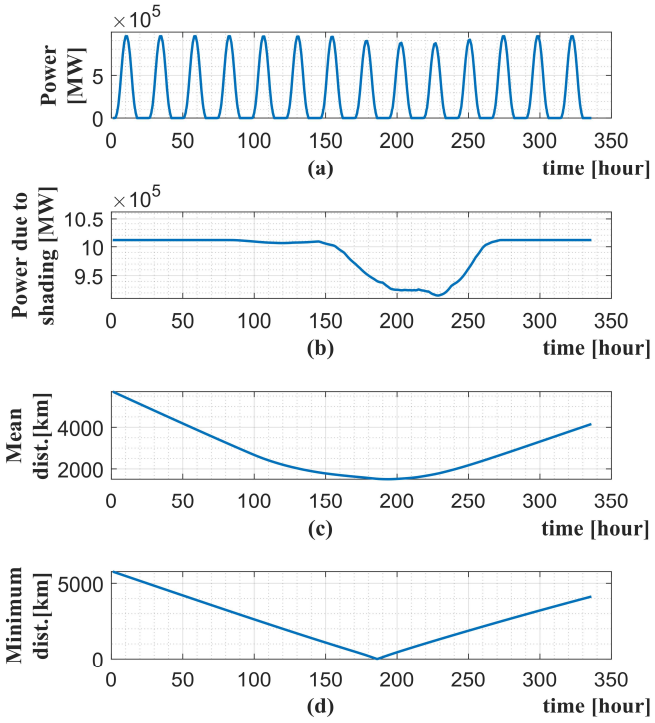

Figure 11. Hurricane over trajectory #7 passing through PV plants of the U.S.-Caribbean super grid.

Figure 12 shows the individual power profiles of the PV solar plants in the U.S.-Caribbean super grid. The black color curve is the aggregated power profile of all PV solar plants. This arithmetical aggregation of individual PV power profiles is only possible assuming that all PV plants of the Central and North Caribbean islands and the contiguous U.S. territory are injecting power to the same interconnected U.S.-Caribbean super grid.

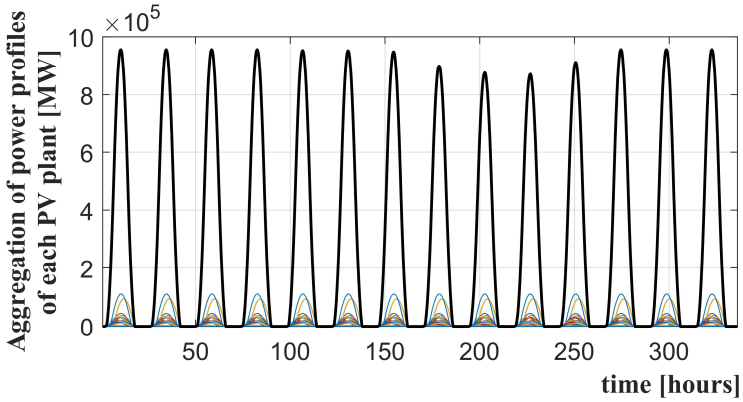

Figure 12. Aggregation of power profiles of each PV solar power plant in the U.S.-Caribbean super grid.

3.4. U.S.-Caribbean-South America super grid

In this scenario, the simulation covers the impact of hurricane on PV solar power plants with the U.S.-Caribbean super grid extended to South America. This scenario is thus called U.S.-Caribbean-South America super grid and requires a submarine power interconnector between Florida and The Bahamas and the extension of the U.S.-Caribbean super grid from Puerto Rico to the islands of the South Caribbean and reaching to South America. Trinidad and Tobago are connected to the Guyana by a high voltage power interconnector. The purpose of this scenario is to assess the potential extra-benefit of large-scale integration of the Caribbean super grid with both the U.S. and South America. This work aims at assessing the overall reduction of spatiotemporal power variability, and ultimately compare the power smoothing performance.

Figure13(a) shows the total power profile generated by the PV power plants of the U.S.-Caribbean-South America super grid under the spatiotemporal impact of hurricane shading. The impact of the hurricane is observed mostly between time 160 h and 260 h in the PV plants located in the contiguous US. However, a very small power variability is also observed between times 75 h to 140 h.

Figure 13(b) shows the reduction of PV power capacity due to hurricane shading effect mostly between time 160 h and 260 h. The power valley from the hurricane over the Caribbeans keeps relatively negligible as compared Florida and the U.S. East coast because the power capacity in the US East coast is more robust than in the Caribbeans.

Figure 13(c) shows the mean geometric distance of all PV solar plants to the hurricane eye. This curve indicates how close in average the PV solar plants are to the hurricane.

Figure 13(d) shows the PV solar plant in West Florida with the closest distance from the hurricane eye at time 189 h.

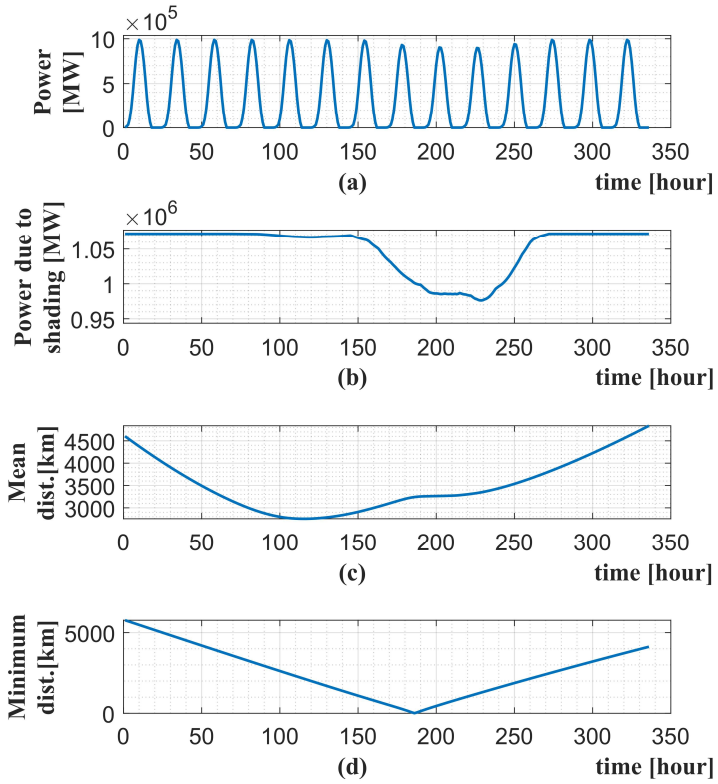

Figure 13. Hurricane over trajectory #7 passing through PV plants of the U.S.-Caribbean-South America super grid.

Figure 14 shows the individual power profiles of the PV solar plants in the U.S.-Caribbean-South super grid. The black color curve is the aggregated power profile of all PV solar plants. This arithmetical aggregation of individual PV power profiles is only possible assuming that all PV plants are injecting power to the same interconnected U.S.-Caribbean-South America super grid.

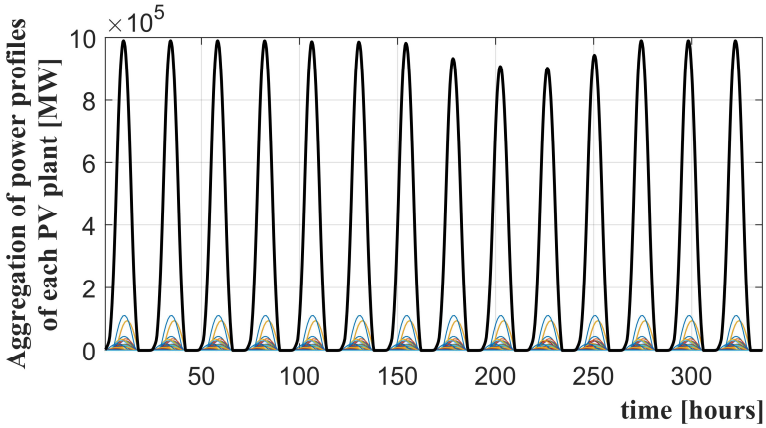

Figure 14. Aggregation of power profiles of each PV solar power plant in the U.S.-Caribbean-South America super grid.

3.5. All trajectories into U.S.-Caribbean-South America super grid

In this scenario, the PV power plants in the U.S.-Caribbean-South America super grid are impacted by all ten parabolic synthetic hurricane trajectories, shown on **Figure 2**. The purpose of this scenario is to identify the trajectory with higher peak power variability. To plot the PV solar power, shading and power valley profile curves of all ten trajectories, an algorithm was implemented in MATLAB to open the data files of simulation results and plot altogether in a single figure. The algorithm was detailed in the **Figure 4**(b) and the all-trajectories curves are shown in **Figure 15** and **Figure 16**.

Figure 15(a) shows the power profiles of all PV power plants in the U.S., Caribbean, and the southern countries of South America in ten different synthetic hurricane trajectories. **Figure 15**(b) shows the hurricane shading effect on the total PV power capacity. **Figure 15**(c) shows the magnitude of power valley for each hurricane trajectory. Power valley occurs when the hurricane is spatially close to high density of PV power capacity, maximizing the shading as shown in **Figure 15**(b) and the irradiance is instantaneously in its maximum at noon, as shown in **Figure 15**(a). For example, a hurricane passing through PV plants but at midnight will not produce power valley, since at midnight it is not expected any PV solar power. The power valley in **Figure 15**(c) is obtained by searching the local minimum of the overall power profile presented in **Figure 15**(a).

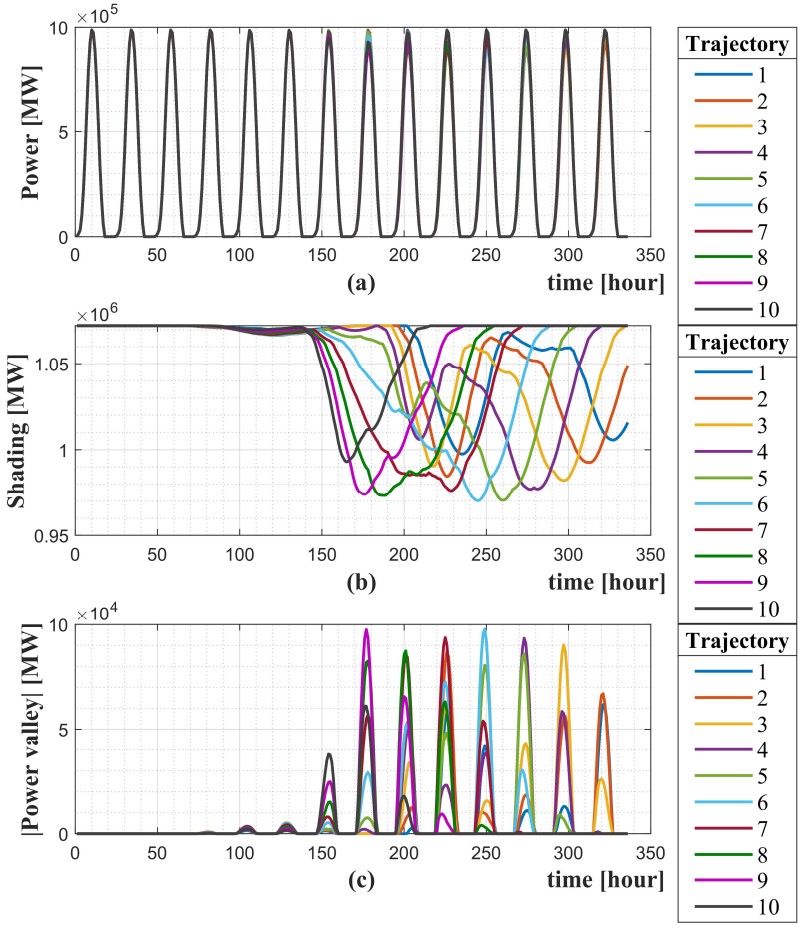

Figure 15. (a) Total PV power profile, (b) Shading on PV power plant capacity, and (c) Power valley.

The power profile and shaded capacity on PV plants located in the Caribbeans and South America are negligible because the total PV capacity in the Caribbeans is very small as compared to the contiguous US power grid, and because South America are outside the hurricane's corridor.

This work is restricted by a set of assumptions and scope limitations to make feasible a study of a large-scale grid under a multitude of intermittent and unpredictable variables.The simulation results on this subsection, associated to a specific scenario, is comparatively discussed in the subsection 3.7 together with other scenarios.

3.6. All trajectories into standalone Caribbean super grid

In this scenario, the PV power plants in the Caribbean super grid are impacted by all ten parabolic synthetic hurricane trajectories, shown on **Figure 2**. This scenario neither includes PV plants on the contiguous US power grid nor the extension to south Caribbean islands and South America. The simulations results were obtained using the algorithm shown in the **Figure 4**(b). The purpose of this scenario is to assess magnitude of power variability exclusively on the standalone Caribbean super grid to allow later comparison of smoothing performance with the U.S.-Caribbean-South America super grid investigated in the previous scenario.

Figure 16(a) shows the power profiles of all PV power plants in the standalone Caribbean super grid in ten different synthetic hurricane trajectories. **Figure 16**(b) shows the hurricane shading effect on the total PV power capacity. **Figure 16**(c) shows the magnitude of power valley for each hurricane trajectory. Power valley occurs when the hurricane is spatially close to high density of PV power capacity, maximizing the shading as shown in **Figure 16**(b) and the irradiance is instantaneously in its maximum at noon every 24 hours, as shown in **Figure 16**(a). The power valley in **Figure 16**(c) is obtained by searching the local minimum of the overall power profile presented in **Figure 16**(a).

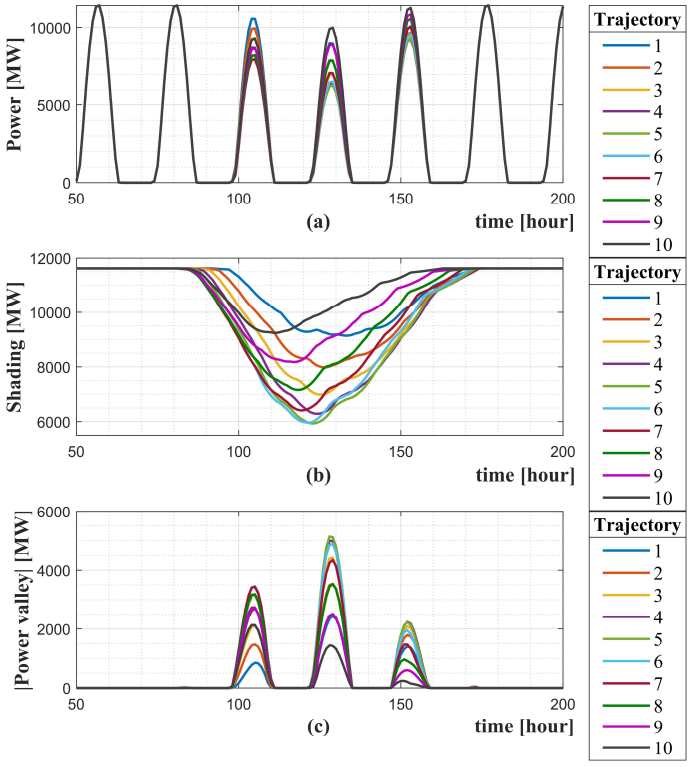

Figure 16. (a) Total PV power profile, (b) Shading on PV power plant capacity, and (c) Power valley.

The shaded capacity on PV plants located in the Caribbeans reduces more significantly from 11,600 MW (100%) to 6,000 MW (52%) over trajectory # 5 than the 9,250 MW (80%) power capacity valley in trajectory #10. The reason for this strong power decay can

be explained by **Figure 17**, which shows trajectory #5 in proximity to most of the PV plants in the Caribbeans, between time 90h and 170h.

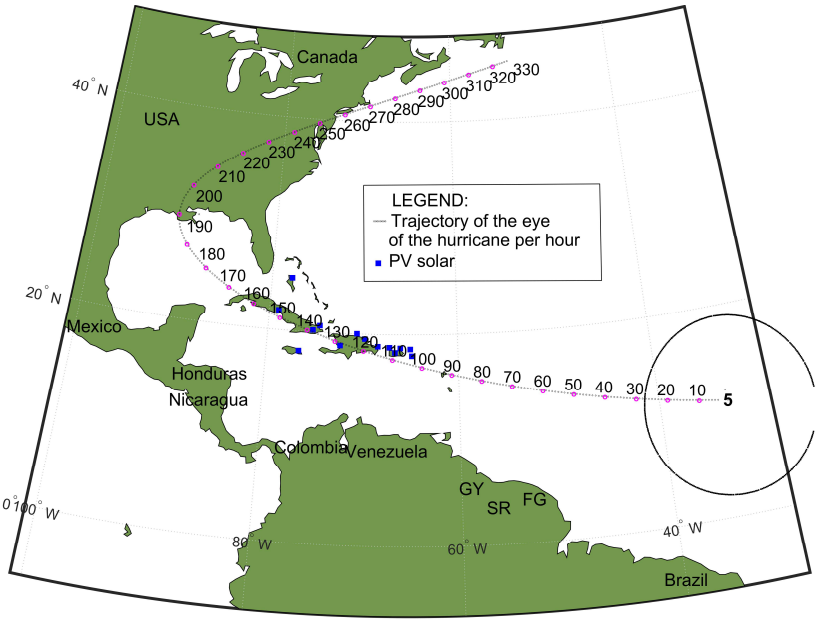

Figure 17. Hurricane over trajectory #5 passing through PV plants of the Caribbean super grid.

The simulations presented the practical capabilities of the proposed spatiotemporal method for PV power profile estimation, investigated the impact of the hurricane on PV plants connected in four schemes of super grid interconnectivity, and generated a multitude of PV power profile curves in single or multiple hurricane trajectories. However, a deep understanding of the power variability impact of the hurricane on each super grid scheme demands the consolidation of results for a comparative analysis of scenarios.

3.7. Comparative analysis of scenarios

The power variability is defined and estimated by the following indicators [20]:

$$\Delta P_{min} = \frac{P_{pre-hurrican} - P_{min}}{P_{pre-hurricane}} \quad (13)$$

where $P_{pre-hurricane}$ is the peak power at the first noon, while the hurricane has not shaded PV power plants, and P_{min} is minimum local peak of the power profile under hurricane shading.

Table 5 shows the power variability of PV plants under shading caused by a hurricane over trajectory #7 in four scenarios of super grid interconnectivity. The power values are obtained from **Figure 6**, **Figure 9**, **Figure 11**, and **Figure 13**. Minimum local peak P_{min} occurs in two occasions: (a) over the Caribbeans from time 90 h to 160 h, and (b) over the contiguous US territory from time 150h to 330h. PV power valley does not occur over South America because this region is far away from the hurricane's corridor.

Table 5. Power variability during hurricanes in different scenarios of super grid interconnectivity.

Values	Standalone U.S. power grid	Standalone Caribbean super grid	U.S.-Caribbean super grid	U.S.-Caribbean-South America super grid
Trajectory number	#7	#7	#7	#7
Total number of PV solar plants	36	14	50	90
Total PV capacity [MW]	1,000,000	11,623	1,011,623	1,072,335
Figures	**Figure 6** and **Figure 7**	**Figure 9** and **Figure 10**	**Figure 11** and **Figure 12**	**Figure 13** and **Figure 14**
Power valley in the Caribbeans:	-	-	-	-
$P_{pre-hurricane}$ [MW]	N.A.	11,463	955,983	989,600
P_{min} [MW]	N.A.	7,135	952,087	985,563
ΔP_{min} [%]	N.A.	37.8%	0.4%	0.4%
Power valley in the contiguous U.S.:		-	-	-
$P_{pre-hurricane}$ [MW]	946,114	N.A.	955,983	989,600
P_{min} [MW]	861,819	N.A.	871,316	901,893
ΔP_{min} [%]	8.9%	N.A.	8.9%	8.9%

Table 5 consolidates the assessment of power variability ΔP_{min} to support the comparison of scenarios of super grid interconnectivity. In the standalone Caribbean super grid scenario, the power valley ΔP_{min} is 37.8%. In the U.S.-Caribbean super grid and the U.S.-Caribbean-South America super grid scenarios, the power valley ΔP_{min} significantly reduces to 0.4% and 0.4%, respectively. The reason for high percentual power valley in standalone Caribbean super grid as compared to the U.S.-Caribbean super grid and U.S.-Caribbean-South America super grid can be explained by the large hurricane shading area covering the entire small area of the standalone Caribbean super grid in the same instant. In this scenario, there is no interconnection with U.S. and South America power grids, which would otherwise collectively absorb part of the impact of hurricane shading in the Caribbeans. It can be concluded that the Central and North Caribbean islands (including U.S. territories of Puerto Rico and U.S. Virgin Islands) have much to benefit from the interconnection to the contiguous U.S. grid or both contiguous U.S. and South America grid. With such interconnections, the North Caribbean islands can access PV power from areas not within the hurricane's corridor. For example, the most western American states (California, Oregon, Nevada, and Utah, South America are not in the route of the hurricanes corridor.

In the scenarios of Standalone U.S. power grid, U.S.-Caribbean super grid, and U.S.-Caribbean-South America super grid, the power valley ΔP_{min} in the contiguous U.S. is lower than 9%. The power valley in the contiguous U.S. is dominantly determined by the large PV power capacity of the contiguous U.S. projected to 2050, which is approximately fourteen times the total PV capacity of the other countries and territories in the Caribbean super grid and the extension to South America.

Table 6 shows the power valley produced by hurricanes in all ten trajectories. In general, US states with higher geospatial density of PV capacity has higher power valley because they have more PV capacity to be shaded by the hurricane. Trajectory #10, for example, has the second lowest power valley because the trajectory passes off the coast of Florida. The western part of Texas is on the trajectory #1 and is not much populated with PV power capacity, as shown in **Figure 2** and **Figure 5**. For this reason, a hurricane over

trajectory #1 produces moderate power variability. Such interpretation based on spatial PV density by U.S. states should be used with caution because *ROCI* onshore is 463 km in the simulations, possibly shading two or more U.S. states. Table 6, in column 4, shows the minimum instantaneous power valley of **Figure 15**(c) of hurricanes in ten synthetic parabolic trajectories. Instantaneous power valley includes the daily variability of solar irradiance cycle. The time (night or day) that the hurricane passes over the PV plant plays an important role in the magnitude of the instantaneous power valley. For example, a hurricane over an PV plant at night does not produce shading impact on a PV plant since the output is anyway zero at night.

The power capacity valley is the equivalent reduction of PV capacity due to hurricane shading, disregarding the effect of solar cycle. The power capacity variability during hurricanes is shown in **Figure 15**(b).

Table 6 organizes the power valleys in ascending order, placing their ordering values in parenthesis in columns 4 and 5. **Table 6** shows that a strong decline in capacity power due to hurricane shading does not mean that the instantaneous power valley is also deep. Louisiana State, hit by a hurricane in trajectory #5, experience a relatively shallow instantaneous power valley despite having the second deepest capacity power valley. The reason for shallow instantaneous power valley is the hurricane approaching the PV plants at midnight, alleviating the impact of shading during the day before and after, as show in trajectory #5 of **Figure 18**. At midnight, the instantaneous power valley is zero because the hurricane shading cannot reduce the PV power that is already zero due to the lack of solar irradiance. The percentual capacity power valley is also calculated in reference to the pre-hurricane peak power $P_{pre-hurricane}$ is 989,600 MW in **Figure 15**(a).

Table 6. Power valley produced by hurricanes hitting U.S.-Caribbean-South America super grid.

Trajectory #	States	Spatial density of PV capacity [MW/km2]	Instantaneous Power Valley [MW]	Capacity Power Valley [MW]	Capacity Power Valley [%]
1	Texas	0.0193 (2)	63,156 (2)	66,700 (1)	6.7%
2	Texas	0.0193 (2)	88,851 (9)	79,690 (3)	8.1%
3	Texas	0.0193 (2)	85,178 (5)	90,150 (4)	9.1%
4	Louisiana	0.0025 (3)	88,455 (7)	95,130 (5)	9.6%
5	Louisiana	0.0025 (3)	78,304 (3)	101,850 (9)	10.3%
6	Alabama	0.0013 (4)	88,563 (8)	102,110 (10)	10.3%
7	Florida	0.0460 (1)	87,707 (6)	96,090 (6)	9.7%
8	Florida	0.0460 (1)	81,970 (4)	98,880 (8)	10.0%
9	Florida	0.0460 (1)	90,249 (10)	98,130 (7)	9.9%
10	Off the coast of Florida	0 (5)	55,656 (1)	79,310 (2)	8.0%

Counterintuitively, a hurricane hitting Alabama, the state with the lowest spatial density of PV plants, causes the stronger shading impact on PV plants capacity among other states. A plausible explanation for this is because a hurricane with shading impact radius of approximately 1.3 times *ROCI* (1.3 x 463 km) hitting Alabama, in the middle of the U.S. South Coast, can cover large portions of PV plants in the East side (Florida and Georgia), and some plants in the West side (Louisiana).

An important insight of this analysis is that the spatial planning for PV plant siting regarding hurricane conditions should consider locations with minimum capacity power valley, not spatial density by U.S. state, and not instantaneous power valley. The time that the hurricane approaches a PV power plant, which defines the shape of the instantaneous power valley, is not a variable under human control. Being conservative in practice,

instantaneous power valley incorporating solar cycle is not useful for planning or design, which should focus on the worst-case scenario.

The next analysis focus on the impact of all ten trajectories of hurricane shading on the standalone Caribbean super grid. Standalone Caribbean super grid takes a much smaller geospatial footprint than the U.S.-Caribbean-South America super grid. The density of PV capacity by each island is not much relevant since they are small as compared to the dimensions of the hurricane and surrounded by vast portions of the Caribbeans Sea. Being a spatially remote island but also electrically interconnected to a super grid are a major advantage because the power valley locally generated in the island, is punctually well absorbed by the super grid.

Table 7 shows the magnitude of power valley from the simulation curves of **Figure 19**. The deepest power valley occurs on trajectory #5. Most western and eastern trajectories, trajectories #1 and #10, respectively, produce less power valley due to the long distance to the PV power plants. The percentual capacity power valley is also calculated in reference to the pre-hurricane peak power $P_{pre-hurricane}$ is 11,463 MW in **Figure 16**(a).

Table 7. Power valley produced by hurricanes hitting standalone Caribbean super grid.

Trajectory #	Instantaneous Power Valley [MW]	Capacity Power Valley [MW]	Capacity Power Valley [%]
1	2,414	2,325	20.3%
2	3,543	3,482	30.4%
3	4,439	4,477	39.1%
4	5,026	5,177	45.2%
5	5,145	5,530	48.2%
6	4,891	5,500	48.0%
7	4,329	5,051	44.1%
8	3,515	4,306	37.6%
9	2,754	3,288	28.7%
10	2,143	2,223	19.4%

Table 7 shows capacity power valley up to 48.2% in the standalone Caribbean super grid. Comparing with a non-grid connected PV plant under hurricane shading analyzed in **Figure 18**, presenting a power capacity valley of 88%, the interconnection of the islands of the Caribbeans in a super grid would bring significant reduction on power variability.

In general, there are not many options to improve geospatial distribution of PV plants in the Caribbean islands. PV plants are normally installed onshore and most of the islands are close to each other. However, plenty of geospatial distribution possibilities are available in the vast contiguous U.S. territory.

For PV planning purposes, the capacity power valley is the most appropriate reference for the planning and design of super grids or energy storage capacity since it is not sensitive to the time that a hurricane is expected to pass over the PV power plants, i.e., a stochastic variable modeling the instantaneous power valley profile.

Comparing **Table 7** and **Table 6**, the capacity power variability is 48.2% in the standalone Caribbean super grid as compared to just 10.3% in the for the U.S.-Caribbean-South America super grid. From exclusive power variability perspective, the interconnection of the standalone Caribbean super grid to the U.S. and South America is advantageous to the Caribbeans.

The comparative analysis confirms that large-scale interconnectivity schemes such as the proposed U.S.-Caribbean-South America super grid sustain lower power variability than local interconnectivity schemes.

A spatiotemporal method dedicated to assessing the impact of hurricanes on PV solar power generation was proposed, and its functionalities were demonstrated in a cases-

study of four possible future scenarios for a large-scale interconnectivity scheme in the Caribbean region.

Four interconnectivity schemes investigated in this research are:

- Standalone contiguous US power grid: The US is projected to reach 1,000,000 MW in 2050, significantly exceeding the forecasted 72,335 MW for the Caribbean and northern countries and states in South America. In this scenario, the power variability of the standalone contiguous US power grid is not sensitive to hurricanes over the Caribbean.
- Standalone Caribbean super grid: Without interconnection to the US or South America grid for power valley filling, a standalone Caribbean super grid would endure the most significant power valley among all schemes. This is primarily due to the arrangement of PV plants on a chain of closely situated islands, nearly entirely covered by the shading caused by hurricanes. Additionally, the trajectories of hurricanes typically align parallel to the axis of the Caribbean islands chain, prolonging the duration of their impact. Given the projected Caribbean PV capacity by 2050, which is negligible compared to that of the US, the Caribbean region would derive substantial benefits from either a U.S.-Caribbean interconnector or a Caribbean-South America interconnector.
- U.S.-Caribbean super grid: The U.S.-Caribbean super grid significantly reduces power variability during hurricanes passing over the Caribbean. The integration of the overseas US territories of Puerto Rico and the US Virgin Islands into an integrated U.S.-Caribbean super grid proves beneficial in mitigating local power valleys.
- U.S.-Caribbean-South America super grid: This interconnectivity scheme adds approximately 60,712 MW of PV capacity, primarily from Brazil (58,500 MW), situated outside the hurricane corridor. Extending the U.S.-Caribbean super grid does not significantly reduce the overall relative power variability. More PV solar power capacity or other renewable energy source (e.g., wind or hydropower) in South America would be needed to significantly smooth the power variability in hurricane-prone areas. Connecting the U.S.-Caribbean super grid to South America would provide energy security by an alternative power supply in the event of disconnection of segment of the Caribbean super grid.

The analysis of the geospatial scenario with all hurricane trajectories reveals that the proposed spatiotemporal method for PV power profile estimation is a valuable tool for PV solar power planning, forecasting, and design because it provides a generalized, flexible, long-distance, long-term, and multi-variable comprehensive understanding of the impact of hurricanes.

4. Analysis of consistency

This research adopts the Ceferino's model for hurricane shading, which was previously validated in [3]. Then, this research builds upon the Ceferino's model a complementary method to address the need of forecasting PV solar generation in large-scale super grids. The focus of this research is primarily the delivery a method to forecast the PV solar generation profile under hurricanes with the integration of islanded high voltage grids into different topologies of super grids.

However, this proposed algorithm for spatiotemporal estimation of power profile was shrunk from MW to kW magnitude in this analysis to confirm the consistency of the estimated power profile with power measurements in a 200 kW-scale PV plant in Fort Lauderdale, FL, hit by hurricane Katrina (2005), investigated in [2]. According to Cole et al., during hurricanes, the resulting PV solar power profile reduces to 18% to 60% of the initial clear sky conditions [2].

Figure 18 shows in black color the power profile estimation using the spatiotemporal method proposed in this research for hurricane Katrina, making first landfall in Florida. The red dashed profile is the power profile measured by Cole et al. [2]. Hurricane Katrina

made landfall initially near the Miami-Dade/Broward County line as category-1 during the evening of August 25, 2005, at 22:00 h, according to reports of the National Hurricane Center and the National Centers for Environmental Information [36], [37]. The y-axis was intentionally maintained in MW to not modify the scale of the spatiotemporal algorithm, which is originally designed to simulate large-scale super grids.

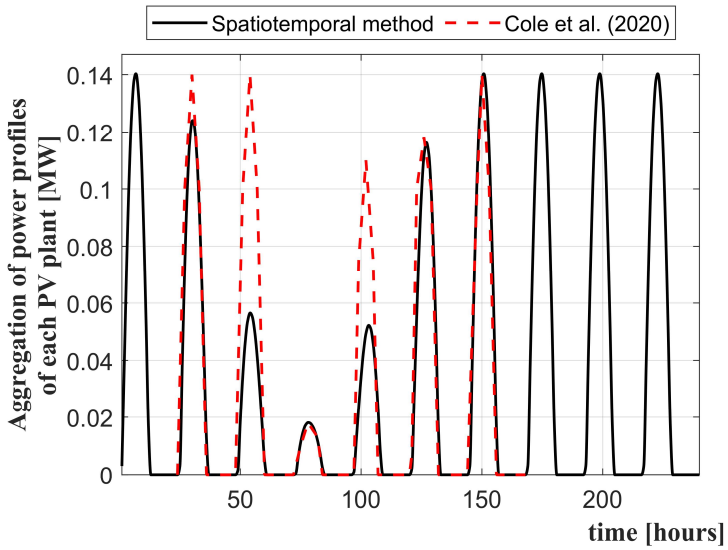

Figure 18. Power profile by the spatiotemporal method (in black) and the power measured on a PV plant in Fort Lauderdale, FL for Aug 22-29, 2005 [2].

The rated power capacity in direct current kW (the PV modules capacity) in practice is higher than the alternating current PV solar plant rated capacity, by a factor called inverter load ratio. The inverter load ratio of the 200 kW dc PV generation studied by Cole et al. can be calculated by [2]:

$$ILR = \frac{P_{dc\,rated}}{P_{ac\,rated}} = \frac{200\ kWdc}{140\ kWac} = 1.43 \quad (14)$$

The spatiotemporal method for PV solar power profile estimation proposed in this research, which utilizes alternating current rated power, were simulated assuming $P_{ac\,rated}$ of 140 kW ac to obtain the peak power at noon in pre-hurricane conditions.

Table 8 shows the parameters of hurricane Katrina for the spatiotemporal power profile estimation.

Table 8. Parameters of hurricane Katrina (2005).

Parameters	Description	Katrina (2005)	Sources
C	hurricane category	1 (in Florida)	[36]
a_1	slope factor	1.97	[3]
a_2	slope factor	0.0965	[3]
b_1	short-distance correction factor	1.15	[3]
b_2	short-distance correction factor	-0.126	[3]
c_1	scale factor	2.48	[3]
c_2	scale factor	-0.139	[3]
$ROCI$	radii of the outermost closed isobar	150 nautical miles (277 km)	[37]

for onshore			
$ROCI$ for offshore	radii of the outermost closed isobar	130 nautical miles (241 km)	[37]
d, R, and f	absolute distance from hurricane eye, relative distance from hurricane eye, and functional form	recalculated after each hurricane step	-
Δt_h	simulation time step	1 h	[16],
V_{tr}	hurricane translational speed	4.11 – 5.14 m/s (8 – 10 knots)	[37]
-	trajectory shape	parabola crossing the border of Broward/Miami-Dade County, FL	[16], [36]

Figure 19 shows the synthetic parabolic trajectory simulating the point of impact of hurricane Katrina (2005) using the spatiotemporal estimation method proposed in this research.

Figure 19. Hurricane simulating first point of impact of hurricane Katrina (2005), and PV plant in Fort Lauderdale, FL.

Figure 20 shows simulations of a 140 kW ac PV plant in Fort Lauderdale. **Figure 20**(a) shows the spatiotemporal solar power estimation profile in blue color obtained by the spatiotemporal method, and the measurements of power on a PV plant in Fort Lauderdale in red dashed line, informed by Cole et al. [2]. **Figure 20**(b) shows the power capacity valley caused by the hurricane passage. **Figure 20**(c) and (d) have similar distance profile as the hurricane approaches the PV plant, because the mean distance in this specific scenario is calculated over a single PV plant.

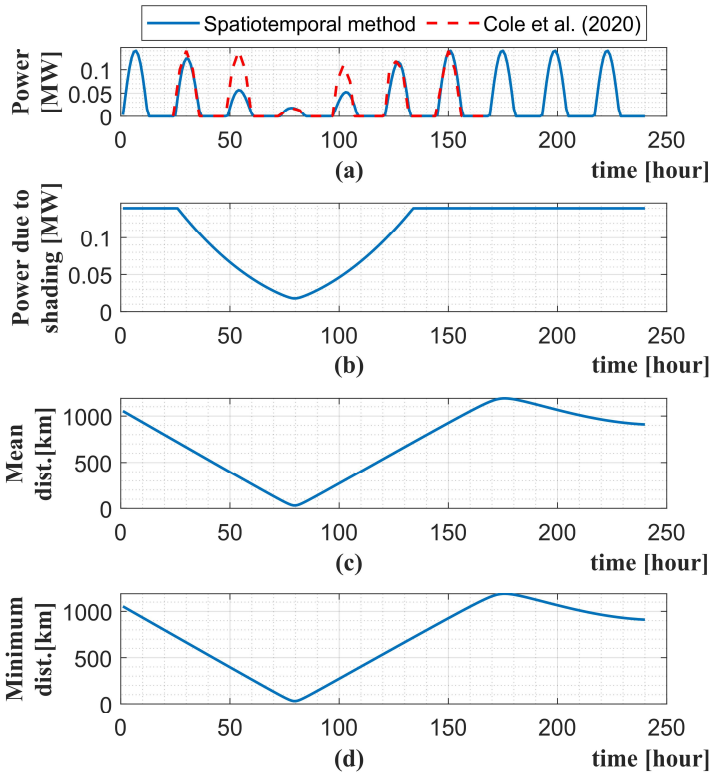

Figure 20. Katrina-like hurricane passing over 140 kW ac PV plant in Fort Lauderdale, FL.

Table 9 presents an analysis of consistency of the proposed spatiotemporal method for estimation of PV power profiles under hurricane in reference to Cole et al. measurements [2].

Table 9. Comparative analysis of proposed spatiotemporal method and existing technical literature.

Method	Spatiotemporal method	Cole et al.'s measurements [2]	Difference:
Number of days under shading	5	3	2
Pre-hurricane power [kW ac]	140 (100%)	140 (100%)	0
Day 1's noon peak power [kW ac]	123.8 (88%)	140 (100%)	-16.2
Day 2's noon peak power [kW ac]	56.5 (40%)	140 (100%)	-83.5
Day 3's noon peak power [kW ac]	18.1 (13%)	18 (13%)	0.1
Day 4's noon peak power [kW ac]	52.1 (37%)	110 (79%)	-57.9
Day 5's noon peak power [kW ac]	113.2 (81%)	118 (84%)	-4.8
Peak average [kW ac]	72.7 (52%)	82.0 (59%)	-9.3 (-6.6%)

The 5-days average power obtained from this research simulations reached 52% average power drop from pre-hurricane conditions, which is in the range of 18% to 60% reported by Cole et al. [2]. Also, the minimum power drop obtained by the spatiotemporal simulations reached 18.1 kW which is identical to Cole et al.'s measurements, which indicated 18 kW minimum.

Unfortunately, the exact coordinate (latitude and longitude) of the PV power plant was not indicated in Cole et al.'s simulations [2]. For this reason, the comparison of day-by-day peak power does not reflect the same spatiotemporal conditions. However, the modeling of hurricane shading using Ceferino's model, formulated on equation (2), leads

to 360° symmetrical shape of hurricane shading, also observed in **Figure 1** and **Figure 8**. This symmetry is not observed on Cole et al.'s simulations [2].

The spatiotemporal method estimated 5 days of shading while the Cole et al.'s simulations [2] indicate just 3 days during the passage of the hurricane Katrina over a PV plant in Fort Lauderdale, FL. The number of shaded days is also related to the time the hurricane stays over the PV plant, which is dependent on the translational speed of the hurricane. The simulations of this research adopted the speed values from NOAA [37].

The spatiotemporal method for estimation of PV power profile under hurricanes is based on empirical shading equations with 360° symmetric shape, as show in **Figure 1** and equations (1), (2), and (3). The formulated proposal and validation of the shading equations (1), (2), and (3), was demonstrated by Ceferino et al., in 2021, by observation of best proposed equation fitting producing minimum Akaike Information Criterion (AIC) score [3]. Despite selection of best fitting, the stochastic simulation of GHI under hurricanes showed differences between Ceferino's model and Cole's model [3][2].

In contrast to the Ceferino's model [3], which is admitted supporting spatiotemporal forecasting of irradiance only, this research focus on forecasting PV solar power generation profile, which is useful to support electrical power engineering studies, specifically time-series power flow of super grids. However, this spatiotemporal method for estimation of PV power profile does not aim at substituting power flow methods. This research method is a bridge and facilitates the connection of PV irradiance forecasting into the electrical power systems studies. It aggregates the power profile of each PV plant connected in a super grid, supporting basic analysis about power variability in large blocks of power. Also, this method is an interdisciplinary tool that generates input (PV solar power profile) for time-series power flow studies.

5. Conclusions

This section summarizes the contributions, limitations of this research, and outlines topics for future investigation.

5.1. The contributions of this research

Intermittent renewables operating in extreme weather events produce high variability of power generation profile. Deployment of massive amounts of battery energy storage systems to damp local power variability is a very expensive solution. This research instead proposes a large-scale interconnection of local power grids by high voltage submarine power cables, known as super grids. The simulation results indicate that the PV power variability in the Caribbean super grid under hurricanes is lower when it is connected to the U.S. contiguous power grid or South America. Reducing intermittent renewable power variability is critical in the transition to the decarbonization of the power sector because power consumers expect high levels of service without power interruptions. This research demonstrates that the U.S.-Caribbean-South America super grid or U.S.-Caribbean super grid are alternative solutions to address the power variability in PV power plants under hurricanes.

Another contribution of this research is that the proposed spatiotemporal method for estimation of PV power profile covers a gap for the complete understanding of the impact of hurricanes on renewables. The most significant weather-dependent renewables are wind and PV power. While the method to estimate wind power under the impact of hurricane have been investigated [20][16], the estimation of large-scale PV power under hurricanes has been poorly studied. This proposed method for PV estimation covers this gap in the literature.

The proposed spatiotemporal method for estimating PV power profiles is both comprehensive and versatile. It was implemented in MATLAB coding and programmed to generate the curves and the map of the hurricane trajectory. By synthesizing a set of ten parabolic trajectories, the method effectively encompasses a significant portion of the hurricane corridor extending from the Caribbean Sea to the Gulf of Mexico. By modeling the

hurricane trajectory over a period of 10 to 14 days, the method more accurately captures the long-distance physical reality of a hurricane. The application of this method yields outcomes with international implications. In essence, the method is specifically tailored for studies on large-scale super grids. Such versatility and comprehensiveness are not normally found on data-driven methods.

One important merit of this work is that the proposed method is an indispensable tool for future time-series power flow simulations of large-scale PV systems under extreme hurricanes. It is indispensable because it provides spatiotemporal PV power profile estimations that can be injected on bus nodes for comprehensive power systems simulations in realistic extreme weather conditions. Hurricanes causes PV power valley, but it is unrealistic to assume that the massive expansion of renewables and associated intermittency should be backed up by unlimited production of batteries. Bulk interconnectivity schemes, as proved in the standalone Caribbean super grid scenario study, can reduce PV power valleys during hurricanes from 37.8% to 8.9%, as shown on Table 5. Further methods and software tools are needed to support future comprehensive time-series power flow studies of power systems with high levels of renewables operating in extreme weather conditions.

5.2. Limitations of this work and future work

This method was based on parametric modeling of hurricane shading, based on equations empirically fitted and validated by Ceferino et al. [3]. The contribution of this proposed method for super grid simulation builds over the parametric equations elaborated by Ceferino et al. [3], but also adds novel elements such as the modeling of parabolic multi-trajectories, and simulation of multiple PV plants in different interconnectivity schemes of a proposed super grid. This research adopts parametric modeling to find flexibility to study a hurricane in a multitude of trajectories with the aim of obtaining an overall understanding of the spatiotemporal impact of hurricanes on PV generation interconnected to super grids.

Future data-driven method may find more accurate results studying a specific hurricane hitting a specific spot for validation of specific PV power plant. The choice for parametric modeling was made to analyze hurricanes from the broad perspective of large-scale PV capacity distributed in a multitude of countries in the Caribbeans, South America and the US. Future alternative data-driven methods can find more accurate power estimation for specific or synthetic hurricane trajectory. This research found few literatures available to make feasible the complete validation of the proposed method over a distribution of PV solar capacity over all countries in the Caribbeans, some countries of South America and the US. A future data-driven method would be a much-needed effort for the advancement of renewable energy science.

As for the scope limitation, this proposed method for estimation of PV power profile does not intend to substitute power flow algorithms. This method intends to support more in-depth and comprehensive conclusions generated by future power flow studies of the Caribbean super grid and possible extended interconnections. A comprehensive analysis of the time-series power flow on the proposed super grid can investigate hybrid systems with other renewable energy sources such as wind power. Wind turbines generate a surplus peak power during hurricanes [16].

Another restriction of the scope of this work is the analysis of techno-economic feasibility since this method is in the incipient phase of basic studies. A comparison of the cost-benefit of the proposed interconnected Caribbean super grid, incorporating wind power assessment versus an alternative topology with large-scale batteries is a potential topic for future investigations. Uncertainty and sensitivity analysis of different scenarios are potential topics for future research. Further innovative and alternative methods for technical justification of the US-Caribbean-South America super grid and other scenarios can be investigated by the scientific community in future studies.

Finally, another interesting topic for future studies is the estimation of wind and solar power in the U.S.-Caribbean-South America super grid also in non-hurricane conditions in all seasons.

Author Contributions: Conceptualization, R.I.; methodology, R.I.; software, R.I.; writing—original draft preparation, R.I.; formal analysis, R.I., N.S., and S.G.D.S.; investigation, R.I.; data curation, R.I.; validation, S.G.D.S.; writing—review and editing, R.I., N.S., T.K. and S.G.D.S.; supervision, N.S. and T.K.; project administration, T.K.; funding acquisition T.K.. All authors have read and agreed to the published version of the manuscript.

Declaration of competing interest: The authors declare no conflicts of interest.

Funding: This manuscript is based upon work supported by the US Department of Energy, under contract number DE-AC05-00OR22725.

Data Availability Statement: Data are contained within the article.

Appendix A

The main input parameters and the procedure to obtain the solar irradiance absorbed by the fixed tilted PV solar plants in clear sky conditions are [23]:

- L : Latitude of the PV plant
- LOD: Longitude of the PV plant
- N: day number 258, corresponding to September 15, in the middle of the US hurricanes season.
- The remaining variables are described on the list of abbreviations (Appendix C).

Calculation of the time difference with reference to GMT [23]:

$$T_{GMT} = round\left(\frac{LOD}{15^\circ}\right) \quad \text{(A1)}$$

Calculation of angle of declination (δ_s) [23]:

$$\delta_s = 23.45^\circ \sin\left[\frac{2\pi}{365}(N-81)\right] \quad \text{(A2)}$$

Calculation of B and EoT [23] [39]:

$$B = \frac{2\pi}{365}(N-81) \quad \text{(A3)}$$

$$EoT = 2.292 * (0.0075 + 0.1868 * cos(B) - 3.2077 * sin(B) - 1.4615 * cos(2 * B) - 4.089 * sin(2 * B)) \quad \text{(A4)}$$

Calculation of $LMST$ [23]:

$$LMST = 15^\circ\, T_{GMT} \quad \text{(A5)}$$

Calculation of solar time correction (TC) [23]:

$$TC = \begin{cases} -4^\circ\,(LMST - LOD) + EoT, & if\ LOD \geq 0^\circ \\ 4^\circ\,(LMST - LOD) + EoT, & if\ LOD < 0^\circ \end{cases} \quad \text{(A6)}$$

Calculation of sunrise and sunset hour angle time (ω_{ss} and ω_{sr}) [23]:

$$\omega_{ss} = cos^{-1}(-\tan L\,.\tan\delta) \quad \text{(A7)}$$

$$\omega_{sr} = \omega_{ss} \quad \text{(A8)}$$

Calculation of sunset solar time with correction (AST_{ss} and T_{ss}) [23]:

$$AST_{ss} = \frac{\omega_{ss}}{15^\circ} + 12h \quad \text{(A9)}$$

$$T_{ss} = AST_{ss} + |TC| \quad \text{(A10)}$$

Calculation of sunrise time with correction (AST_{sr} and T_{sr}) [23]:

$$AST_{sr} = \frac{\omega_{sr}}{15^\circ} - 12h \quad \text{(A11)}$$

$$T_{sr} = AST_{sr} + |TC| \quad \text{(A12)}$$

Calculation of solar time (Ts) [23]:

$$LST = LT + \frac{TC}{60} \quad \text{(A13)}$$

Calculation of $\sin\alpha$ [23]:

$$\sin\alpha = \sin L \,.\sin\delta + \cos L \,.\cos\delta \,.\cos\omega \quad \text{(A14)}$$

Calculation of hour angle degree (ω_s) [23]:

$$\omega_s = 15^\circ\,(AST - 12h) \quad \text{(A15)}$$

Calculation of extraterrestrial solar energy flux (A) [23]:

$$A = 1160 + 75\,sin\left[\frac{360}{365}(N - 275)\right] \quad \text{(A16)}$$

Calculation of factors k and C [23]:

$$k = 0.174 + 0.035\,sin\left[\frac{360}{365}(N - 100)\right] \quad \text{(A17)}$$

$$C = 0.095 + 0.04\,sin\left[\frac{360}{365}(N - 100)\right] \quad \text{(A18)}$$

Calculation of solar irradiation on horizontal surface:

Calculation of available beam radiation in the sky ($G_{B.norm}$) [23]:

$$G_{B.norm} = A.\,e^{\frac{-K}{sin\propto}} \quad \text{(A19)}$$

$$G_B = G_{B.norm}\,sin\propto \quad \text{(A20)}$$

Calculation of diffuse solar irradiation (G_D) [23]:

$$G_D = C\,.G_{B.norm} \quad \text{(A21)}$$

Calculation of total irradiation (G_T) [23]:

$$G_T = G_B + G_D \quad \text{(A22)}$$

Calculation of solar irradiation on tilt surface:

It is assumed that the tilt angle (β) is the same as the latitude (L) [23].

$$\beta = L \quad \text{(A23)}$$

Calculation of R_B, R_D and R_R [23]:

Liu and Jordan model define R_B as [38] [23]:

$$R_B = \frac{\cos(L-\beta)\,.cos\delta\,.\sin\omega_{ss} + \omega_{ss}.\sin(L-\beta).\sin\delta}{\cos L\,.cos\delta\,.\sin\quad_{ss} + \omega_{ss}.\sin\quad.\sin\delta} \quad \text{(A24)}$$

The equations adopted by commonly adopted for calculation of R_D and R_R are [23]:

$$R_D = \frac{1+\cos\beta}{2} \quad \text{(A25)}$$

$$R_R = \frac{1-\cos\beta}{2} \quad \text{(A26)}$$

Calculation of Irradiation ($G_{B,\beta}$, $G_{D,\beta}$, G_R) [23]:

$$G_{B,\beta} = G_B \times R_B \quad \text{(A27)}$$

$$G_{D,\beta} = G_D \times R_D \quad \text{(A28)}$$

$$G_R = G_T \times \rho \times R_R \quad \text{(A29)}$$

where the ground Albedo (ρ) is assumed to be 0.3, as in [23].

Calculation of Total irradiation absorbed by fixed tilted PV module ($G_{(T,\beta)}$) [23]:

$$G_{T,\beta} = G_{B,\beta} + G_{D,\beta} + G_R \quad \text{(A30)}$$

where: $G_{B,\beta}$ is the beam solar irradiation by fixed tilted PV module, $G_{D,\beta}$ is beam solar irradiation by fixed tilted PV module, and G_R is the reflected solar irradiation.

Appendix B

Table B shows PV capacity distributed in 48 U.S. states, and 26 Brazilian states.

Table B. PV power capacity of U.S. and Brazil.

U.S. States	Cumulative PV capacity [MW ac] [40]	Latitude, Longitude	Brazil States	Cumulative PV capacity [MW ac] [41]	Latitude, Longitude
California	30,738	36.232171, -119.916045; 34.795990, -118.446496; 35.382405, -120.058481	Minas Gerais	6,468	-17.127722, -43.844568
Texas	13,404	31.095329, -102.344823; 30.241752, -97.513868 29.217125, -95.658233 30.706400, -96.068545	Bahia	2,402	-12.598216, -44.106217
Florida	7,838	27.763334, -82.234079 30.515422, -86.514052 30.449714, -83.198413 30.289455, -82.777271	Piaui	3,050	-10.098598, -45.258506
North Carolina	6,371	36.027904, -80.300748 36.027838, -80.300811 34.223174, -77.945766	Sao Paulo	1,162	-21.295295, -49.935380
Arizona	4,806	33.266410, -111.616842	Ceara	1,536	-3.988918, -38.393514
Nevada	4,008	35.787342, -114.959010	Pernambuco	1,158	-9.070659, -38.146141
New York	3,906	42.750417, -73.760531	Rio Grande do Norte	1,383	-5.566330, -37.028634
Georgia	3,676	31.415000, -84.836573 32.999522, -85.035689	Paraiba	811	-6.840431, -36.930855
New Jersey	3,413	40.334604, -74.646582	Rio Grande do Sul	23	-29.663366, -50.589770
Massachusetts	3,257	42.445847, -72.622222 42.402297, -71.007982	Mato Grosso	22	-15.285470, -56.267769
Virginia	3,032	36.792318, -76.668125 37.960675, -75.555078	Parana	16	-25.341358, -49.094838
Colorado	2,154	38.626906, -104.663352	Para	16	-3.224113, -52.255189
Utah	2,001	39.843394, -111.884718	Roraima	14	2.815288, -60.683043
Illinois	1,815	40.081691, -88.243801	Espirito Santo	13	-19.402187, -39.990263
South Carolina	1,602	32.878153, -79.972821	Santa Catarina	12	-26.824511, -52.221743
Maryland	1,496	39.112493, -75.963808	Mato Grosso do Sul	11	-21.927429, -54.867826
Minnesota	1,309	45.097138, -93.644808	Tocantins	6	-10.145414, -48.316027
Hawaii	-	Not contiguous US	Rio de Janeiro	5	-21.266003, -41.761048
New Mexico	1,173	35.048635, -106.529196	Goias	5	-15.385015, -49.090919
Louisiana [42]	345	30.676825, -91.392683	Amapa	4	-0.002117, -51.083712
Mississippi [42]	300	30.676447, -91.392408	Alagoas	4	-9.571945, -35.771952
Alabama [42]	175	30.675551, -91.391077	Maranhao	2	-3.591578, -43.937995
Tennessee [42]	150	32.510525, -89.730594	Roraima	2	2.815280, -60.683045
Others	12,039	41.233289, -110.753551	Acre	1	-10.010626, -67.759293
			Distrito Federal	1	-15.781504, -48.122397
			Amazonas	1	-2.636500, -60.949138
			Sergipe	1	-10.984704, -37.054391
Total PV	109,008 MW	in Dec 2022 [40][42]	Total PV	18,129 MW	in Oct 2023 [41]
Total PV	1,000,000 MW	projected to 2050 [31]	**Total PV**	58,500 MW	projected to 2050 [35]

The location of the aggregated power capacity of each North American and Brazil's states are distributed to the coordinates indicated. These coordinates were visually obtained using Google Maps search for the most representative existing "PV solar plants" in each state. This geospatial attribution of coordinates by state was assumed to limit the computational cost and the total simulation processing time, without compromise on the accuracy of power profile results. The PV power capacity of US states located in the path of hurricanes were obtained from [42]. The power capacity of the US state indicated as others is allocated to the state of Wyoming (outside the hurricanes corridor), to not interfere as power valley in the estimation of PV power profile under hurricanes shading.

Appendix C

Table C. List of Abbreviations.

A	W/m²	Extraterrestrial solar energy flux
a_1	-	Hurricane shading slope factor
a_2	-	Hurricane shading slope factor
a_3	-	Parabola coefficient
ρ	-	Albedo
AST	h	Apparent or true solar time
B	rad	Equation of time (relative to the day number N in the year)
b_1	-	Hurricane shading short-distance correction factor
b_2	-	Hurricane shading short-distance correction factor
b_3	-	Parabola coefficient
β	°	Tilt angle of PV module
c_1	-	Hurricane shading scale factor
c_2	-	Hurricane shading scale factor
c_3	-	Parabola coefficient
C	-	Hurricane category
d	km	Distance to the hurricane eye.
δ^h	-	Global Horizontal Irradiance (GHI) Decay
δ_s	°	Angle of declination
ΔP	%	PV solar power variability
EoT	minutes	Difference between apparent and mean solar times
f	-	Functional forms
F_d	%	Fossil fuel dependence factor
F_e	%	PV expansion factor
f_{PV}	-	Derating factor of PV cell
GHI	kW/m²	Global Horizontal Irradiance
G_B	kW/m²	Beam solar irradiation by collector on a horizontal surface
$G_{B.norm}$	kW/m²	Beam solar irradiation in the sky
G_D	kW/m²	Diffuse solar irradiation
G_R	kW/m²	Reflected solar irradiation
G_{STC}	kW/m²	Incident radiation at standard test conditions (equal to 1 kW/m²)

$G_{T,\beta}$	kW/m²	Total solar irradiation absorbed by fixed tilted PV module
γ	1/°C	Temperature coefficient of PV panel (3.5 × 10−3 1/°C),
I	p.u.	Irradiance for per unit calculation in clear sky
I^h	%	Clearness factor
L	°	Latitude of the PV plant
LOD	°	Longitude of the PV plant
$LMST$	°	Local mean sidereal time, degrees
N	day	Day number in a year
NOAA	-	National Oceanic and Atmospheric Administration
$P_{pre-hurricane}$	MW	PV power in pre-hurricane conditions
P_{min}	MW	Minimum instantaneous peak PV power
$P_{PV,rated}$	MWac	Photovoltaic power capacity
P_{total}	MW	Total power capacity of a country
PV	-	Photovoltaic
R	km	Relative distance to the hurricane eye
$ROCI$	km	Radius of outermost closed isobar.
R_B	%	Ratio between global solar energy on a horizontal surface and global solar energy on a tilted surface.
R_D	%	Ratio between diffuse solar energy on a horizontal surface and diffuse solar energy on a tilted surface.
R_R	%	Factor of reflected solar energy on a tilted surface
T_a	°C	Ambient temperature (in °C)
TC	°C	Solar time correction
T_{cell}	°C	PV cell temperature (in °C)
$T_{cell,STC}$	°C	PV cell temperature at standard test conditions (equal to 25 °C)
T_{GMT}	h	Time difference with reference to GMT
T_{sr}	h	Time of sunrise with correction
T_{ss}	h	Time of sunset with correction
ω_s	°	Hour angle degree
ω_{sr}	°	Sunrise hour angle time
ω_{ss}	°	Sunset hour angle time
x	°	Latitude of hurricane eye in parabola trajectory
y	°	Longitude of hurricane eye in parabola trajectory

References

1. Méndez-Tejeda, R.; Hernández-Ayala, J. J. Links between climate change and hurricanes in the North Atlantic. *PLOS Clim* **2023**, 2(4), e0000186. https://doi.org/10.1371/journal.pclm.0000186.
2. Cole, W.; Greer, D.; Lamb, K. The potential for using local PV to meet critical loads during hurricanes. *Solar Energy* **2020**, 205, 37-43. https://doi.org/10.1016/j.solener.2020.04.094.
3. Ceferino, L.; Lin, N.; Xi, D. Stochastic modeling of solar irradiance during hurricanes. *Stoch Environ Res Risk Assess* **2022**, 36, 2681–2693. https://doi.org/10.1007/s00477-021-02154-2.

4. IEA. Electricity Grids and Secure Energy Transitions; International Energy Agency: Paris, **2023**; License: CC BY 4.0. Available online: https://www.iea.org/reports/electricity-grids-and-secure-energy-transitions (Accessed Oct 19, 2023).
5. Bompard, E.; Fulli, G.; Ardelean, M.; Masera, M. It's a Bird, It's a Plane, It's a...Supergrid!: Evolution, Opportunities, and Critical Issues for Pan-European Transmission. *IEEE Power and Energy Magazine* **2014**, 12(2), 40-50. https://doi.org/10.1109/MPE.2013.2294813.
6. Bastianel, G.; Ergun, H.; Van Hertem, D. A Multi-GW Energy Hub for Southern Europe: the Mediterranean Energy Island Proposal. *2023 AEIT HVDC International Conference* (AEIT HVDC), Rome, Italy, **2023**, pp. 1-6. https://doi.org/10.1109/AEITHVDC58550.2023.10179006.
7. Ahmed, T.; Mekhilef, S.; Shah, R.; Mithulananthan, N. Investigation into transmission options for cross-border power trading in ASEAN power grid. *Energy Policy* **2017**, 108, 91-101. https://doi.org/10.1016/j.enpol.2017.05.020.
8. Itiki, R.; Manjrekar, M.; Di Santo, S. G.; Machado, L. F. M. Topology Design Method for Super Grids based on experiences in China and North America. 2020 *IEEE Power & Energy Society Innovative Smart Grid Technologies Conference* (ISGT), **2020**, Washington, DC, USA, pp. 1-5. https://doi.org/10.1109/ISGT45199.2020.9087768.
9. Xu, Z.; Dong, H.; Huang, H. Debates on ultra-high-voltage synchronous power grid: the future super grid in China?. *IET Gener. Transm. Distrib*. **2015**, 9, 740-747. https://doi.org/10.1049/iet-gtd.2014.0281.
10. Ardelean, M.; Minnebo, P. The suitability of seas and shores for building submarine power interconnections. *Renewable and Sustainable Energy Reviews* **2023**, 176, 113210. https://doi.org/10.1016/j.rser.2023.113210.
11. Purvins, A.; Sereno, L.; Ardelean, M.; Covrig, C.-F.; Efthimiadis, T.; Minnebo, P. Submarine power cable between Europe and North America: A techno-economic analysis. *Journal of Cleaner Production* **2018**, 186, 131-145. https://doi.org/10.1016/j.jclepro.2018.03.095.
12. Namjil, E.; Komoto, K. Strategies for Implementing of Very Large Scale Solar and Wind Power Plants in the Gobi Desert for the Northeast Asia Regional Energy Market. *2022 IEEE 49th Photovoltaics Specialists Conference* (PVSC), **2022**, Philadelphia, PA, USA, pp. 1179-1181. https://doi.org/10.1109/PVSC48317.2022.9938502.
13. Kim, H.; Jung, T. Y. Embarking on the Asia Supergrid: Trade impact of carbon pricing on regional sustainability in northeast Asia. *Renewable and Sustainable Energy Reviews* **2023**, 183, 113426. https://doi.org/10.1016/j.rser.2023.113426.
14. Itiki, R.; Manjrekar, M.; Di Santo, S. G. Technical feasibility of Japan-Taiwan-Philippines HVdc interconnector to the Asia Pacific Super Grid. *Renewable and Sustainable Energy Reviews* **2020**, 133, 110161. https://doi.org/10.1016/j.rser.2020.110161.
15. Ramachandran, S.; Siala, K.; de La Rúa, C.; Massier, T.; Ahmed, A.; Hamacher, T. Life Cycle Climate Change Impact of a Cost-Optimal HVDC Connection to Import Solar Energy from Australia to Singapore. *Energies* **2021**, 14(21), 7178. https://doi.org/10.3390/en14217178.
16. Itiki, R.; Manjrekar, M.; Di Santo, S. G. Proposed Extension of the U.S.–Caribbean Super Grid to South America for Resilience during Hurricanes. *Energies* **2024**, 17(1), 233. https://doi.org/10.3390/en17010233.
17. Vera, N. A.; Ríos, M. A. Planning a Latin America SuperGrid: A First Approach. *2018 IEEE ANDESCON*, Santiago de Cali, Colombia, **2018**, pp. 1-5. https://doi.org/10.1109/ANDESCON.2018.8564578.
18. MacDonald, A. E.; Clack, C. T. M.; Alexander, A.; Dunbar, A.; Wilczak, J.; Xie, Y. Future cost-competitive electricity systems and their impact on US CO2 emissions. *Nature Clim Change* **2016**, 6, 526–531. https://doi.org/10.1038/nclimate2921.
19. Ndlela, N. W.; Davidson, I. E. Power Planning for a Smart Integrated African Super-Grid. *2022 30th Southern African Universities Power Engineering Conference* (SAUPEC), Durban, South Africa, **2022**, pp. 1-6. https://doi.org/10.1109/SAUPEC55179.2022.9730631.
20. Itiki, R.; Manjrekar, M.; Di Santo, S. G.; Itiki, C. Method for spatiotemporal wind power generation profile under hurricanes: U.S.-Caribbean super grid proposition. *Renewable and Sustainable Energy Reviews* **2023**, 173. https://doi.org/10.1016/j.rser.2022.113082.
21. Muhs, J. W.; Parvania, M. Stochastic Spatio-Temporal Hurricane Impact Analysis for Power Grid Resilience Studies. *2019 IEEE Power & Energy Society Innovative Smart Grid Technologies Conference* (ISGT), Washington, DC, USA, **2019**, pp. 1-5. https://doi.org/10.1109/ISGT.2019.8791647.
22. Sharpton, T.; Lawrence, T.; Hall, M. Drivers and barriers to public acceptance of future energy sources and grid expansion in the United States. *Renewable and Sustainable Energy Reviews* **2020**, 126. DOI: https://doi.org/10.1016/j.rser.2020.109826.
23. Khatib, T.; Elmenreich, W. Modeling of Photovoltaic Systems Using MATLAB: Simplified Green Codes; 1st ed.; John Wiley & Sons, Incorporated: Newark, 2016.
24. Shahid, Z.; Santarelli, M.; Marocco, P.; Ferrero, D.; Zahid, U. Techno-economic feasibility analysis of Renewable-fed Power-to-Power (P2P) systems for small French islands. *Energy Conversion and Management* **2022**, 255, 115368. Available online: https://doi.org/10.1016/j.enconman.2022.115368.
25. Beven II, L. J.; Berg, R.; Hagen, A. Tropical cyclone report hurricane Michael (AL142018) 7–11 October 2018, National Hurricane Center 17 May (2019). Available online: https://www.nhc.noaa.gov/data/tcr/AL142018_Michael.pdf. (Accessed Jan 01, 2023).
26. Pasch, R. J.; Brown, D. P.; Blake, E. S. Tropical cyclone report hurricane Charley 9-14 August 2004, National Hurricane Center. Available online: https://www.nhc.noaa.gov/data/tcr/AL032004_Charley.pdf. (Accessed Jan 01, 2023).
27. Pasch, R. J.; Blake, E. S.; Cobb III, H. D.; Roberts, D. P. Tropical cyclone report hurricane Wilma 15-25 October 2005, National Hurricane Center, 12 Jan. Available online: https://www.nhc.noaa.gov/data/tcr/AL252005_Wilma.pdf. (Accessed Jan 01, 2023).

28. U.S. Department of Commerce. National Weather Service, North Atlantic Hurricane Tracking Chart 2020. Available online: https://www.nhc.noaa.gov/data/tracks/tracks-at-2020.png (Accessed Oct 17, 2023).
29. Dornan, M.; Shah, K. U. Energy policy, aid, and the development of renewable energy resources in Small Island Developing States. *Energy Policy* **2016**, 98, 759-767. DOI: https://doi.org/10.1016/j.enpol.2016.05.035.
30. CIA. The World Factbook – Explore All Countries; Central Intelligence Agency. Available online: https://www.cia.gov/the-world-factbook/countries/ (Accessed Oct 17, 2023).
31. NREL. Solar Futures Study; National Renewable Energy Laboratory, **2021**. Available online: https://www.energy.gov/sites/default/files/2021-09/Solar%20Futures%20Study.pdf (Accessed Dec 6, 2023).
32. Rakotoson, V.; Praene, J. P. A life cycle assessment approach to the electricity generation of French overseas territories. *Journal of Cleaner Production* **2017**, 168, 755-763. DOI: https://doi.org/10.1016/j.jclepro.2017.09.055.
33. Notton, G.; Voyant, C.; Duchaud, J. L. Difficulties of Solar PV Integration in Island Electrical Networks – Case Study in the French Islands. *E3S Web Conf.* **2019**, 111, 06028. DOI: https://doi.org/10.1051/e3sconf/201911106028.
34. Pillot, B.; Al-Kurdi, N.; Gervet, C.; Linguet, L. Optimizing operational costs and PV production at utility scale: An optical fiber network analogy for solar park clustering. *Applied Energy* **2021**, 298, 117158. DOI: https://doi.org/10.1016/j.apenergy.2021.117158.
35. De Sousa, N. M.; Oliveira, C. B.; Cunha, D. Photovoltaic electronic waste in Brazil: Circular economy challenges, potential and obstacles. *Social Sciences & Humanities Open* **2023**, 7(1), 100456. DOI: https://doi.org/10.1016/j.ssaho.2023.100456.
36. Knabb, R. D.; Rhome, J. R.; Brown, D. P. Tropical Cyclone Report Hurricane Katrina 23-30 August 2005, National Hurricane Center, Jan 4, 2023. Available online: https://www.nhc.noaa.gov/data/tcr/AL122005_Katrina.pdf. (Accessed Jan 01, 2023).
37. NOAA. 2005 Major Hurricane KATRINA (2005236N23285), International Best Track Archive for Climate Stewardship (IBTrACS), National Centers for Environmental Information. Available online: https://ibtracs.unca.edu/index.php?name=v04r00-2005236N23285 (Accessed on Nov 17, 2023).
38. Liu, B. Y. H.; Jordan, R. C. The long-term average performance of flat-plate solar-energy collectors: With design data for the US its outlying possessions and Canada. *Solar Energy* **1963**, 7, 53–74. https://doi.org/10.1016/0038-092X(63)90006-9.
39. Roumpakias, E.; Stamatelos, A. Comparative performance analysis of grid-connected photovoltaic system by use of existing performance models. *Energy Conversion and Management* **2017**, 150, 14-25. https://doi.org/10.1016/j.enconman.2017.08.001.
40. Feldman, D.; Dummit, K.; Zuboy, J.; Margolis, R. Spring 2023 Solar Industry Update, National Renewable Energy Laboratory, April 27, 2023. https://www.nrel.gov/docs/fy23osti/86215.pdf. https://doi.org/10.2172/1974994 (Accessed Oct 25, 2023).
41. ANEEL. Installed Capacity by State, Superintendency of Concessions, Permits and Authorizations for Electrical Energy Services (SCE). Available online: https://app.powerbi.com/view?r=eyJrIjoiNjc4OGYyYjQtYWM2ZC00YjllLWJlYmEtYzdkNTQ1MTc1NjM2IiwidCI6IjQwZDZmOWI4LWVjYTctNDZhMi05MmQ0LWVhNGU5YzAxNzBlMSIsImMiOjR9 (Accessed Oct 17, 2023).
42. Solar Energy Industry Association. Project Location Map, 2023. Available online: https://www.seia.org/research-resources/major-solar-projects-list. (Accessed Oct 17, 2023).